UNIVERSITEIT•STELLENBOSCH•UNIVERSITY
jou kennisvennoot • your knowledge partner

Identity Confidence Estimation of Manoeuvring Aircraft

by

Petrus Jacobus Holtzhausen

Thesis presented at the University of Stellenbosch in partial fulfilment of the requirements for the degree of

Master of Engineering

Division of Applied Mathematics
Department of Mathematical Sciences
University of Stellenbosch
Private Bag X1, 7602 Matieland, South Africa

Study leaders:

Prof. Ben Herbst Prof. Johan du Preez Pieter-Jan Wolfaardt

December 2006

Declaration

I, the undersigned, hereby declare that the work contained in this thesis is my own original work and that I have not previously in its entirety or in part submitted it at any university for a degree.

Signature: .....

P.J. Holtzhausen

Date: .....

Abstract

A radar system observes an aircraft once during each scan of the airspace, and uses these observations to construct a track representing a possible route of the aircraft. However when aircraft interact closely there is the possibility of confusing the identities of the tracks. In this thesis multiple hypothesis techniques are applied to extract an identity confidence from a track, given a set of possible tracks and observations. The system utilises numerous estimation filters internally and these are investigated and compared in detail. The Identity Confidence algorithm is tested using a developed radar simulation system, and evaluated sucessfully against a series of benchmark tests.

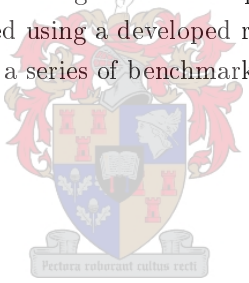

Opsomming

'n Radar sisteem neem 'n vliegtuig waar een keer elke rotasierondte, en skep 'n moontlike pad met behulp van die waarnemings. Indien vliegtuie egter naby mekaar vlieg is daar 'n moontlikheid van identiteitsverwarring. Hierdie probleem word in hierdie tesis ondersoek deur om veelvoudige hipotese tegnieke toe te pas. 'n Waarskynlikheid van 'n vliegpad se identiteit word verkry, gegee die waarnemings en bestaande paaie. Die sisteem gebruik intern 'n aantal estimasie filters en hierdie word in detail ondersoek en vergelyk. Die Identiteits Sekerheid algoritme is deur middel van 'n radar simulasie sisteem getoets en suksesvol geevalueer met 'n reeks toetse.

Acknowledgements

I would like to thank Professor Ben Herbst for his study guidance and Pieter-Jan Wolfaardt from Reutech Radar Systems for giving insight into the nature of radar. I would also like to thank the Reutech Radar Systems company for sponsoring this project.

Dedication

My parents.

Contents

List of Figures

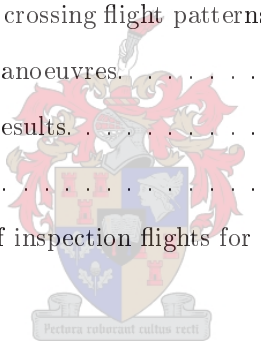

List of Tables

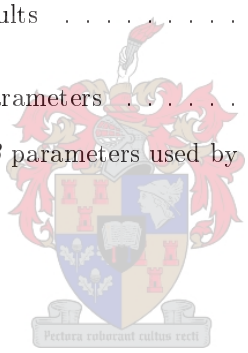

List of Abbreviations

KF	Kalman Filter
$\alpha\beta$	Alpha-Beta Filter
EKF	Extended Kalman Filter
UKF	Unscented Kalman Filter
IFF	Identification Friend or Foe
JPDA	Joint Probabilistic Data Association
MAP	Maximum A Posterior
MHT	Multiple Hypothesis Tracker
PDA	Probabilistic Data Association
GNN	Global Nearest Neighbour
IMM	Interacting Multiple Model
MTT	Multiple Target Tracking
SSR	Secondary Surveillance Radar
RMS	Root Mean Square

List of Symbols

Vectors and Matrices:

c	Speed of light
A	State transition matrix
H	Observation matrix
Q	Process noise covariance
R	Measurement noise covariance
S	Innovation covariance
K	Kalman gain
x	State
$\hat{x}$	Estimated state
P	Process covariance
z	Observation
$\hat{z}$	Estimated observation
μ	Mode probability
Λ	Mode likelihood
M	IMM Mode
Z	Set of measurements
p_{ij}	Markov probability
n_{FK}	Number of false targets

n_K	Number of true targets
D	Number of steps in a track
N	Number of detections in a track
β_{FT}	Probability density for false targets in search volume
β_{NT}	Probability density for new targets in search volume
P_D	Probability of detection
P_{TL}	Probability of track length

Chapter 1

Introduction

Radars operate in a noisy world. It is the task of radar tracking software to keep track of an aircraft, given noisy measurements and aircraft position estimates. This is difficult since the measurements from different aircraft can be mixed and false detections are also a possibility. Sometimes the target remains undetected for undetermined lengths of time causing missed detections.

It is therefore unrealistic to expect a tracker to operate without error indefinitely and identity checking mechanisms are used, for example to ensure that the aircraft that enters the airspace is in fact the aircraft that lands. In aerospace, the aircraft identity is usually confirmed with the use of transponders or by means of radio communication. In military situations however, such aircraft identification is not always possible due to security considerations.

1.1 Problem description

It is sometimes unavoidable for aircraft to manoeuvre close to one another, causing situations where identity confirmation is not straightforward. In combat situations radio silence is usually enforced, and chase planes tasked to confirm a target's identity by sight often needs to execute close quarters flight patterns.

Thus in case of non-operational identity confirmation systems, it is necessary to ascertain to what extent two closely encountering aircraft could have been confused with one another. Figure 1.1 illustrates a scenario involving two confirmed aircraft with end positions supplied by a tracker. After the close encounter in the region of uncertainty, the two aircraft A and B arrive at positions A' and B'. It is the task of the tracker to decide whether aircraft A and B ends up at positions A' and B' respectively or vice versa.

Since no tracker can do this with certainty, it is useful to provide a confidence measure of a specific track to a radar operator. The idea is to provide additional information to aid human judgement during difficult decision making.

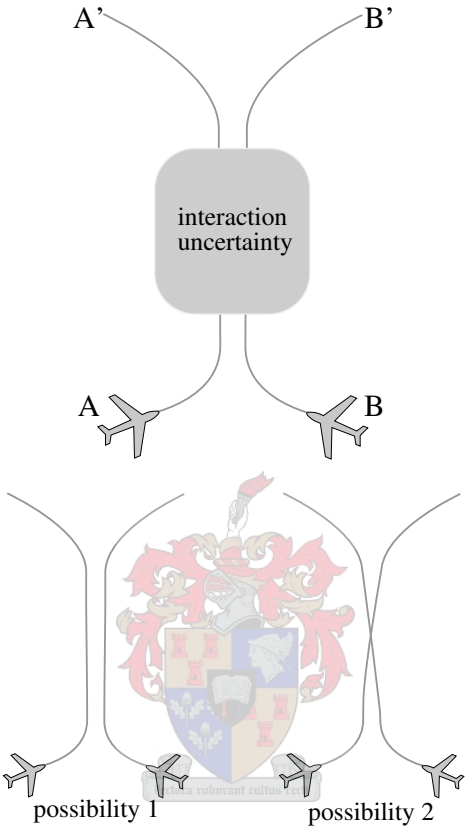

Figure 1.1: The interaction of two flight paths

1.2 Problem analysis

Two aircraft can easily be confused after a close encounter as the result of radar noise, false detections and missed detections. The following factors play a role in this problem and can aid us in the finding of a solution:

- Noisy observations and radar characteristics: The radar site location and noise parameters largely determine the extent of the confusion. A useful consideration for example is that radar typical has greater azimuthal error than range error.

- Track history: The movement history of an aircraft is important, and can be used to predict future positions. Past behaviour is also a good indication of future behaviour, for example an aircraft starting a manoeuvre is more likely to be unpredictable than one flying a straight path.
- Physical characteristics and limitations of aircraft and pilot: When engaged in manoeuvre, aircraft dynamics can restrict the kind of motion that can be executed. A pilot can make a 5g turn in combat, but any higher can leave him incapacitated and not combat effective.

Approaching the problem from the radar tracking side, many of these aforementioned factors can be integrated into a single system.

1.3 Literature Study

Radar tracking is a field with many methodologies. The simplest is the Global Nearest Neighbour (GNN) technique [5] that *gates* (i.e. selects) measurements around each track, and then associates each measurement with a track to minimize the sum of measurement-to-track distances.

Bar Shalom is one of the most prominent in this field and is a proponent of Probabilistic Data Association (PDA) [4], where every track is updated by a weighted sum of all observations within the gating window. Special attention needs to be paid to the creation of new tracks and track interaction. Methods like the Joint Probabilistic Data Association (JPDA) are able to handle multiple targets [2].

The Kalman filter of Rudolph Kalman [13] is a good way of estimating aircraft positions, and cope well with noise corrupted observations. The Kalman filter is ubiquitous in the radar tracking world and forms a part of most of the techniques mentioned here.

Reid [16] introduced the Multiple Hypothesis Tracker (MHT) that operates by considering every possibility of data association, and assigning a probability to each hypothesis. Instead of making a hard decision like the other techniques, all possibilities are propagated into the future with the idea that future data will resolve uncertainties. In an MHT hypothesis an estimation filter is associated with each aircraft to give the best possible estimate of position and velocity.

MHT was developed for radar systems, but also has some prominence in optical tracking [8]. In this thesis we mainly make use of Multiple Hypothesis techniques, especially as described by Blackman [5, 6].

1.4 Objectives

The goal of this thesis is to investigate the creation of an identity metric. Given a flight path of an aircraft, radar characteristics and other measurements, what is the confidence that the identity of this aircraft remained preserved throughout the manoeuvre. The method should be able to cope with scenarios involving multiple aircraft possibly performing any kind of manoeuvre.

We will require a simulation system that can simulate typical flight patterns and simulate observations from a radar system. The specifications of the Kameelperd radar from Reutech Radar Systems will be used to simulate a radar system throughout the simulations.

A tracking system will be developed to generate possible tracks. These tracks will be fed to an algorithm to calculate the probability of identity.

1.5 Overview

The thesis builds from simple components up to higher level tracking concepts.

After first covering general **Radar Background**, we investigate estimation filters in the **Track Modeling** section. The performance of various filters like the $\alpha\beta$, Kalman and Interacting Multiple Model (IMM) filter will be compared for different simulated manoeuvres.

The estimation filters will then be integrated with the MHT in the **Track Management** section. Multiple Hypothesis techniques seem promising to handle the desired factors, and we extend it from a normal tracker to serve as an analysis system in **Identity Confidence**. We will simulate the algorithm with a few test scenarios and discuss the software designed.

Chapter 2

Radar Background

Radar (Radio Detection and Ranging) systems form the backbone in the aerospace industry for remotely detecting the position and velocity of objects. Radar uses electromagnetic waves to detect targets by emitting waves from a transmitter and detecting reflected radiation with a receiver. The radar calculates the distance R to the target by measuring the return time Δt of the wave and using the known propagation velocity of electromagnetic radiation

$$R = \frac{c\Delta t}{2}.$$

With the distance to the target known we still need the azimuth and elevation angles to pinpoint a target's position. For rotating antennas the azimuth is the direction in which the antenna is pointing.

2.1 Radar Architecture

The radar system of this study is a mechanically scanned search radar, with a rotating antenna that covers the entire search volume after one rotation. An

Figure 2.1: The Kameelperd radar system simulated in this study.

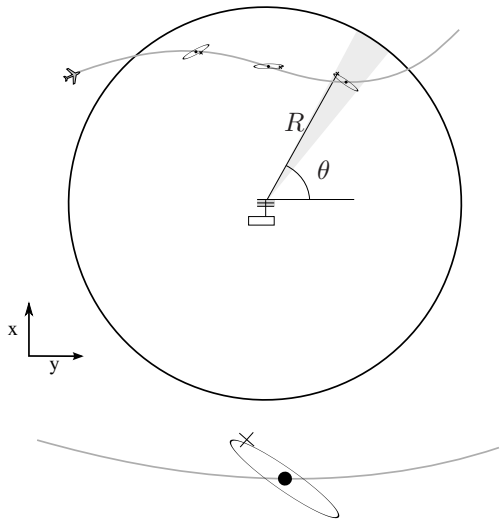

Figure 2.2: View from top of a radar situation, with detail of a noise covariance.

observation (also known as a *hit*) of an aircraft is received once per rotation that typically takes 4 - 10 seconds, and from this a *tracker* creates *tracks* that represent estimated aircraft motion. A functioning radar device of a local company as seen in Figure 2.1 is used for further simulations. This radar has a search volume range of 65 km to a height of 8 km that it covers every 4 seconds. It cannot make height detections, so only azimuthal and range measurements are available. The range is denoted as R and the azimuthal measurement as θ.

2.2 Radar Noise

The radar observations are corrupted by noise as illustrated in Figure 2.2. The noise parameters are known properties of a radar system, for our system an azimuth deviation 0.01222 radians and range deviation of 18m. The azimuth or bearing error is proportional to the target range and therefore plays a greater role in the uncertainty than the range error. The elliptical shape of the error covariance means that tracking flights that move radially away from the radar site is easier than tracking flight orthogonal to the radial.

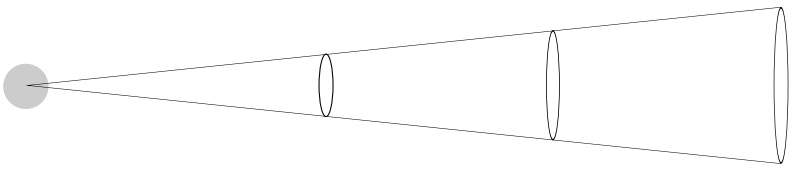

Figure 2.3: Error ellipse proportional to range.

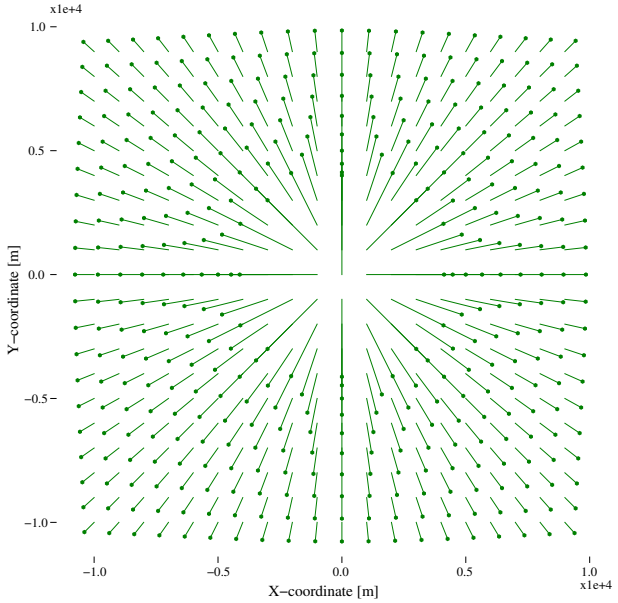

Figure 2.4: The relationship between true and measured position for targets.

As a radar receives reflected electromagnetic waves it also receives a lot of noise from the environment. The received signal needs to score above a certain threshold to qualify as a detected target but it is possible that it could do so in error. Multi-path effects and reflection off stationary objects for example can all lead to *false detections*. This means that the tracker may use the erronous observation to update the track data.

Since search radars typically do not measure elevation, the radial distance R measured is the straight line distance from station to target. The closer the target moves to the station the greater the uncertainty, since the measured position is projected onto x-y plane at distance R in the azimuthal direction θ. This also means that a single (R, θ) measurement can describe various 3d coordinate positions on an arc at distance R from the radar.

Figure 2.4 is a quiver plot illustrating the measurement error of various targets at a height of 4km. The start of the quiver is the x-y coordinates of the original target and the dot is the resulting projection. This effect is less pronounced at distances far away from the station.

2.3 Gating and Correlation

Gating is a method that selects the observations that could possibly be associated with a track. An observation is associated with a track if it is the only

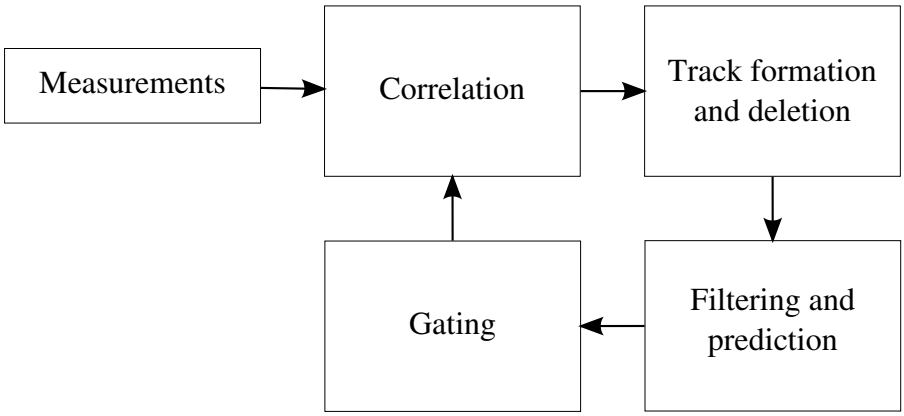

Figure 2.5: Basic multi-target radar tracking system.

measurement within the gating window. The gating window can be rectangular or elliptical and the size may vary according to target behaviour.

If more than one measurement falls in the window it must be decided which measurement associates the best. *Correlation* in this context refers to the process of assigning an observation to a track. This is typically achieved by defining a cost function between the observation and track and attempting to minimize the overall cost of all the associations.

Figure 2.5 illustrates how a gating and correlation plays a role in a basic multi-target tracking system. The tracker creates a new track when an observation does not fall in the gating window of any track. It also deletes a track when a track receives no updates for some time, and it possibly left the search volume. By extrapolating from past observations the tracker constructs a new gating window around a possible future position of an aircraft.

2.4 Typical Aircraft manoeuvres

A helpful part in predicting aircraft motion is to determine what manoeuvres are physically allowed. The maximum airspeed of fighter aircraft can be up to mach 2 [1], and such an aircraft can accelerate and deaccelerate considerably in a linear direction. Turning however remains the greatest source of unpredictable motion. Combat aircraft are capable of performing turns with acceleration forces up to $9g$ [1], but this leaves the pilot incapacitated for the rest of the mission.

Typical g-turns are therefore in the range of 3-5g in fighting situations. Civilian aircraft on the other hand are not expected to make turns exceeding $2g$.

2.5 IFF systems and Transponders

A radar operator only sees blips on the screen from the primary radar, and this is insufficient information to determine the identity of an aircraft. Identification Friend or Foe (IFF) systems are secondary radar systems used to identify aircraft. A base station called a Secondary Surveillance Radar (SSR) continuously sends interrogation signals into airspace. This is received by a transmitter-receiver device outfitted on an aircraft called a *transponder*. The transponder is a radio receiver and transmitter operating on a radar frequency. This device responds to interrogation by the ground station by transmitting a coded reply signal containing aircraft information.

Military systems use high security ciphered modes to thwart enemy interception [15], but usually only over specific zones since broadcasting a signal can be a security risk. Radio silence during combat is the norm. Thus even if an aircraft is identified at a specific moment, its identity might be lost during close encounters with other targets.

Transponders can transmit additional information about the location of an aircraft. Civilian aircraft transmit height information making height detection for Air Traffic Control radars unnecessary. A good multi-target tracking system can integrate data from multiple radars, transponder information and visual sightings to give an accurate representation of what is happening in the air.

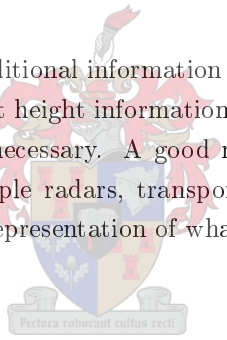

Chapter 3

Track Modeling

The measurements from a radar system are inherently incomplete and noisy. The radar observations could be used as the approximate position of an aircraft, but there is more information available than this noise-corrupted data leading to better estimates. For example the dynamics of an aircraft can be modeled and the typical error a radar system is expected to make is known. All this information can be used to estimate present and future kinematic states such as position, velocity and acceleration.

In this section three methods of filtering will be discussed and compared. The one is an Alpha-Beta ($\alpha\beta$) filter that is currently used by Reutech Radar Systems, the other a Kalman filter that adjusts the gain in an adaptive manner. Lastly the Interacting Multiple Model (IMM) filter merging the results from an ensemble of different filters is described.

3.1 Kinematic model and the Filter

3.1.1 State variable

An aircraft is an object moving through 3d space with an uncertain trajectory, while the observation from the radar is a 2d coordinate pair corrupted by noise. The process is represented by a state variable $\boldsymbol{x}_k$ that is an n-dimensional vector containing components like position, velocity and acceleration at time k.

The dynamic evolution of the system can be described by

$$\begin{aligned} \boldsymbol{x}_{k+1} &= A\boldsymbol{x}_k + v_k \\ \boldsymbol{z}_k &= H\boldsymbol{x}_k + w_k. \end{aligned}$$

where A is the state transition matrix that takes a state from one time step to the next, and H is the observation matrix that converts the state to a measurement value z_k. The term v_k represents the process noise that describes the uncertainty of the aircraft motion. The w_k term represents the measurement noise. Basically it is the error the radar is expected to make.

The choice of components one wishes to include in the state variable, depends on the nature of the problem and the accuracy of modeling that can possibly be achieved.

We use the position, velocity and acceleration components as part of the state vector

$$\boldsymbol{x} = \begin{bmatrix} s_x \\ s_y \\ v_x \\ v_y \\ a_x \\ a_y \end{bmatrix}.$$

Recall that the radar system of our study does not measure height information and we describe the state of the aircraft as a 2D-projection onto the x-y plane.

The following movement equations, with s as position and v as velocity

$$\begin{aligned} \boldsymbol{s}_{k+1} &= \boldsymbol{s}_k + \boldsymbol{v}_k t + \frac{1}{2}\boldsymbol{a}t^2 \\ \boldsymbol{v}_{k+1} &= \boldsymbol{v}_k + \boldsymbol{a_k} t \\ \boldsymbol{a}_k &= a, \end{aligned}$$

translate into the following state transition and observation matrices

$$A = \begin{bmatrix} 1 & 0 & t & 0 & \frac{1}{2}t^2 & 0 \\ 0 & 1 & 0 & t & 0 & \frac{1}{2}t^2 \\ 0 & 0 & 1 & 0 & t & 0 \\ 0 & 0 & 0 & 1 & 0 & t \\ 0 & 0 & 0 & 0 & 1 & 0 \\ 0 & 0 & 0 & 0 & 0 & 1 \end{bmatrix}, \quad H = \begin{bmatrix} 1 & 0 \\ 0 & 1 \\ 0 & 0 \\ 0 & 0 \\ 0 & 0 \\ 0 & 0 \end{bmatrix}.$$

The observation matrix simply converts the state vector into position coordinates. The filter as described is known as a 6-state filter: position, velocity and acceleration each described by 2 components. It is also possible to ignore the acceleration component giving a model that only handles position and velocity. Such a 4-state model gives simpler filter calculations and will handle straight sections with greater accuracy, but fails to follow accelerating manoeuvres.

3.1.2 Choice of tracking coordinates

Our model is described in Cartesian coordinates, because of the simplicity to extrapolate the future state with linear target dynamics. This reduces the computational complexity and makes it possible to use a filter that is linear. There are some disadvantages to this choice however. One disadvantage is the fact that measurement errors are coupled [5, p 55], a fact that needs to be taken into account by the use of independent filters for x and y coordinates.

On the other hand, the use of polar coordinates also perform well in radar systems, and measurements like doppler radar range rate can be easily integrated [5, p 57]. Civilian aircraft movements can be represented as coordinated turns i.e. straight lines and arcs, and [11] shows that the combination of cartesian position with polar velocity components in the state variable give good results. In military environments this is less applicable, because manoeuvres tend to be more sudden and extreme.

Radar measurement errors are often elliptical, and it also makes sense to align the tracking coordinates with the error principal axes of the ellipses to avoid coupling. A popular strategy is to track in mixed coordinates [14]. Here the position is tracked in cartesian coordinates, while the measurement coordinates are aligned to the principal axes of the error ellipse. This technique requires a non-linear tracking filter like the Extended Kalman Filter (EKF). A comparison between the linear filter and the EKF is discussed in [2, p 36]; note from their discussion the failure of EKF performance for larger azimuth errors.

3.1.3 Filtering

The word "filter" as commonly used in signal processing describes the selection of a signal component, typically in the frequency domain. It is a good way to remove unwanted noise, and the removal of noise is in essence what estimation filters also attempt to do. These filters operate in the time domain, not frequency, and they remove noise by predicting the system state and comparing this with actual measurements.

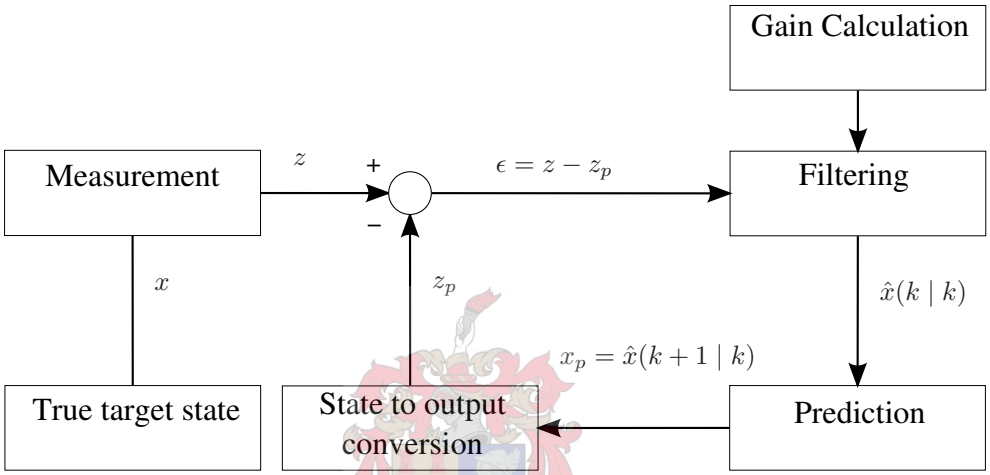

Figure 3.1: Diagram of the estimation filter

Figure 3.1 illustrates the general framework of an estimation filter. The radar observes the target and generates a measurement. This measurement is compared with a predicted measurement generated by extrapolating the current state, and the difference is used to adjust the state for the next time step. A gain parameter, that is perhaps influenced by the error and by other aspects like manoeuvre detection, controls how the error influences the estimate update.

3.2 Alpha-Beta Filter

The Alpha-Beta ($\alpha\beta$) filter is an example of a fixed coefficient filter. It is simple and computationally inexpensive. The process involves making a prediction, and merging this prediction with the received measurement using the gain parameters α and β. This forms the new estimate for the current time step.

The position $\hat{x}$ is estimated as the sum of the predicted position with the prediction error scaled by the fixed coefficient α. The prediction error is the difference

between the received measurement z and the position prediction x_p. The velocity $\hat{v}$ is estimated similarly with use of coefficient β,

$$\hat{x}(k) = x_p(k) + \alpha\,(z(k) - x_p(k)) \tag{3.1}$$

$$\hat{v}(k) = \hat{v}(k-1) + \frac{\beta}{qT}\,(z(k) - x_p(k))\,. \tag{3.2}$$

T represents the time step between measurements. The variable q can be adjusted to handle missed detections, and can be taken as the number of missed scans since last measurement. The future position x_p is now predicted with use of the estimated velocity at time k,

$$x_p(k+1) = \hat{x}(k) + T\hat{v}(k). \tag{3.3}$$

Note that since acceleration is not modeled in the $\alpha\beta$ filter, the predicted velocity is taken as equal to the estimated velocity. This causes poor performance for a target engaged in an accelerating manoeuvre. Another method known as the $\alpha\beta\gamma$ filter [5, p 22] incorporates an acceleration component, and is able to track an accelerating target without steady state error.

3.2.1 Adaptable parameters

An alternative to using an acceleration component, is to vary the parameters according to the behaviour of the target. This is a method that is used by Reutech Radar Systems, and the specific parameter thresholds have been determined experimentally for the radars of their system (Appendix A). Each $\alpha\beta$ parameter pair has an accompanying gating window. Whenever a measurement does not fall within the gating window, the window size and the parameters are increased. It is decreased as future measurements again fall within the window. An advantage of this method is that it also allows the adjusting of the size of the gating window according to the uncertainty in dynamics.

3.3 Kalman Filter

The Kalman filter [13] is a filter that minimizes the expected estimation error $E[|x(k) - \hat{x}(k)|^2]$. Where the $\alpha\beta$ filter has fixed gain coefficients, the Kalman

filter is a recursive filter with the gain continuously adjusted based on the measurements received, the target dynamics and the noise models. Similarly to the $\alpha\beta$ filter, the gain determines to what extent the estimate depends on the measurement or on the dynamic process model.

One of the filter's main strengths is the ease with which it seamlessly combine measurements of different attributes (even possibly from different radar stations) to determine an estimate of the state. It easily deals with missed detections or incomplete sensor data.

The model as developed in Section 3.1 is used. The Kalman filter has two distinct phases, one for prediction and another for update.

Predict

The prediction for the state at time k is made before the measurement is received, by multiplying the state transition matrix A with the previous estimate

$$\hat{x}(k \mid k-1) = A\hat{x}(k-1 \mid k-1).$$

The covariance of the estimated state error is predicted in a similar way, with the process noise covariance Q_k taking into account inaccuracies of the dynamic model

$$P(k \mid k-1) = AP(k-1 \mid k-1)A^T + Q_k. \tag{3.4}$$

Update

The innovation ϵ is the difference between predicted measurement and the actual measurement

$$\epsilon(k) = z(k) - Hx(k \mid k-1). \tag{3.5}$$

The innovation covariance of estimated measurement includes the measurement noise covariance R_k

$$S(k) = HP(k \mid k-1)H^T + R_k. \tag{3.6}$$

The Kalman gain indicates how much the innovation is to affect the state estimate

$$K(k) = P(k \mid k-1)H^T S(k)^{-1}.$$

Now the state estimate is calculated by taking the state prediction and adjusting it according to the innovation and the Kalman gain

$$\hat{x}(k) = \hat{x}(k \mid k-1) + K(k)\epsilon(k). \tag{3.7}$$

The state error covariance estimate (defined as $E[|x(k) - \hat{x}(k)|^2]$, the term that the Kalman filter attempts to minimize) is calculated for time step k with the use of the Kalman gain

$$P(k \mid k) = (I - K(k)H)P(k \mid k-1). \tag{3.8}$$

The Kalman filter is a minimum mean-square error estimator [5, p 25], and is the best solution to the estimation problem, if certain key assumptions hold.

3.3.1 Assumptions

The Kalman filter operates under a series of assumptions [2, p 23] that are not always representative of reality, but still make it useful as an estimation device. Firstly it models linear processes. There are non-linear variations of the Kalman filter as seen in the Extended Kalman Filter, Particle Filter and the Unscented Kalman Filter [12], dependent on the choice of tracking coordinates as explained in Section 3.1.2. These are useful when the initial errors and noise levels are not too large [2]. These are not attributes present in the radar systems of this study so a general linear Kalman filter is used.

The dynamic model of the motion of the aircraft is not an accurate depiction of the true system state, and the Kalman filter introduces a process noise term to represent this error. The process noise is assumed to have a zero mean Gaussian with a known covariance $Q(k)$ as used in Equation 3.4. Similarly the measurement noise is considered a zero-mean Gaussian distribution with a known covariance $R(k)$ as used in Equation 3.6.

3.3.2 Covariances

The functioning of the Kalman filter depends on the choice of the process and measurement covariances Q and R, representing the process noise and measurement noise respectively.

Measurement Noise

The measurement noise covariance of a radar system is a known quantity, since the error that a radar makes can be measured accurately (as seen in Section 2.2). Given the azimuthal and range deviation of a radar system (Appendix A for the radars in this study), it is easy to find the noise covariance associated with a specific measurement.

Figure 3.2 illustrates a typical shape of the measurement covariance, with greater certainty on range than on azimuth. The further the measurement from the centre, the larger the error that is possible (see also Figure 2.3).

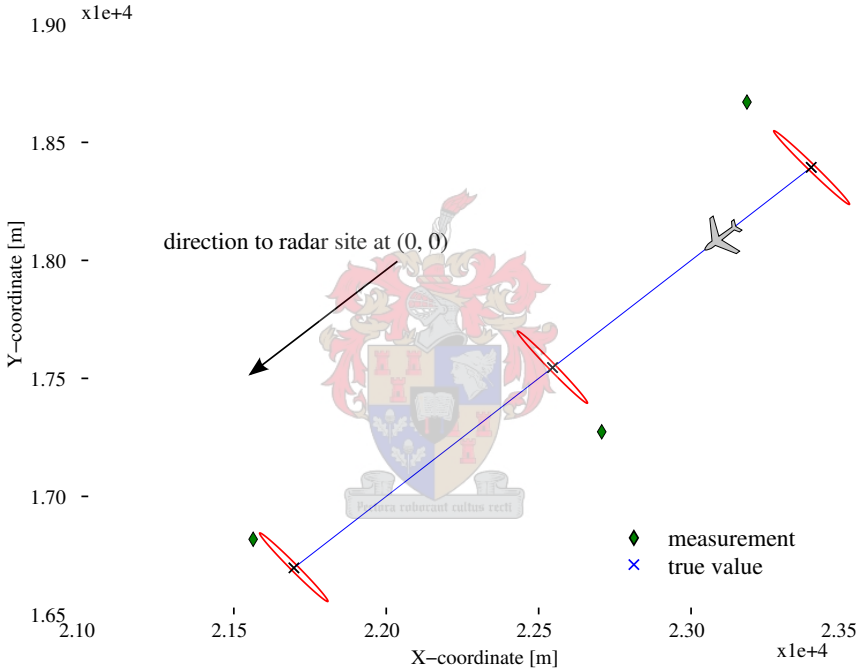

Figure 3.2: Measurement noise covariances

Since the chosen tracking coordinates is Cartesian, the measurement noise needs to be translated from its polar coordinate form. We do this by translating a selection of test points (called sigma points) that define the error ellipse. These sigma points are placed at the centre and at a 1 standard deviation of each principal axis. Figure 3.3 illustrates the placement of point ρ_0 at the centre, with points ρ_1 to ρ_4 bounding the ellipse.

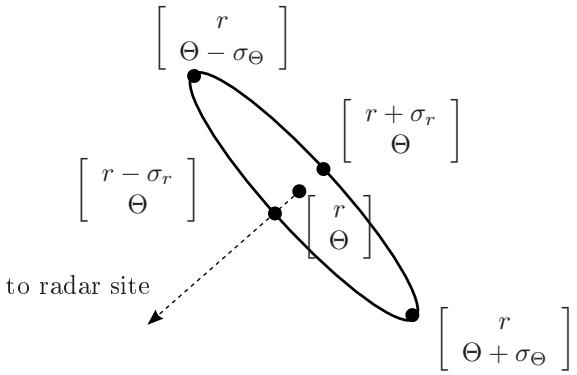

Figure 3.3: Measurement covariance sigma points

The points $\rho_{i,i=0,4}$ are then converted into Cartesian coordinates $p_{i,i=0,4}$ and the covariance can then be calculated

$$\overline{p} = E[p_{i,i=0,4}]$$

$$R = \text{cov}[p_{i,i=0,4}] = E\left[|p - \bar{p}|^2\right].$$

Process Noise

The choice of process noise covariance is not quite as straightforward as finding the measurement noise.

The predictions that the Kalman filter provides is made over short intervals with the use of linear Newtonian dynamics, but this hardly models the mind of a pilot. There is an associated unpredictability involved, and this is represented by the process noise covariance. If aircraft always moved with constant acceleration in straight lines the process noise would be vanishingly small, but in reality (especially in combat situations) a sharp g-turn can be expected at any moment.

Process noise covariance is often considered as a design parameter that is adjusted as a juxtaposition to the more certain measurement noise. Chosen with too large a value the dynamic model is ignored, while with a small value it does not describe the sharp manoeuvre well.

Usually it is chosen by trial and error, but the following physical characteristics provide an indication of what one can expect.

Consider an aircraft flying at a velocity of 500km.h^{-1} with the possibility of executing a range of turns up to $5g$ left or right. Test particles are moved on

trajectories from $1g$ to $5g$ for one scan time of the radar, giving a represention of how much the aircraft motion can differ between the times it can be observed.

The covariance of the test particles' position, velocity and acceleration is now calculated to get an idea of the covariance typical of what to expect. If viewed in a scan time of 4 seconds, the resulting error covariance is quite large. Figure 3.4 illustrates the size of the position covariance.

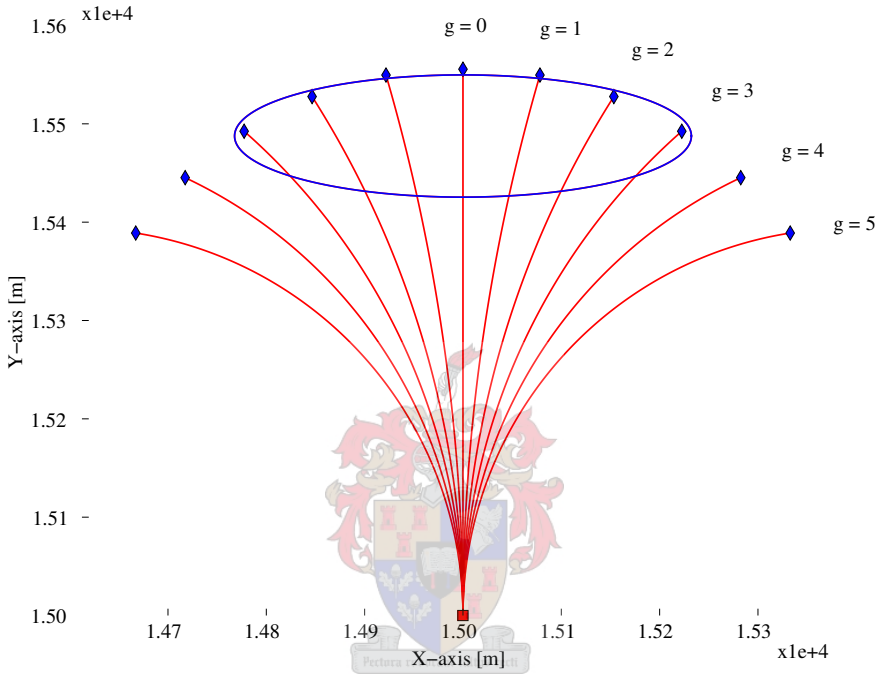

Figure 3.4: Position covariance caused by a set of turns

The covariance Q is elliptical and is influenced by the direction of the aircraft. It is a possibility to let it depend on the estimate of aircraft direction. For the sake of simplicity we approximate it as a diagonal, simmetrical covariance.

This error covariance is basically a worst case scenario, and is large in comparison to the measurement noise. If used it results in a filter that has no confidence in the dynamic model and depends almost exclusively on the measurements. By scaling this covariance one can find a process noise that is representative of the situation yet tuned to make the Kalman filter perform well.

A strategy to be explored in Section 3.4 is to merge the results obtained from multiple filters running in parallel, where each filter has its own process noise aimed to capture a specific scenario.

3.3.3 Kalman Filter Example

During initialisation the estimate covariance P is assigned large values along the diagonal, representing the uncertainty we have about this target and lack of information about its previous motion. This is soon adjusted as more measurements are received and the trajectory becomes available. The Kalman filter may therefore estimate poorly at the start.

Figure 3.5 shows a Kalman filter operating just after initialisation. A prediction (square) is made, with an associated innovation covariance indicated by the larger ellipse. A measurement (diamond) is now received at time step 2, and the state (circle) and state covariance are updated accordingly.

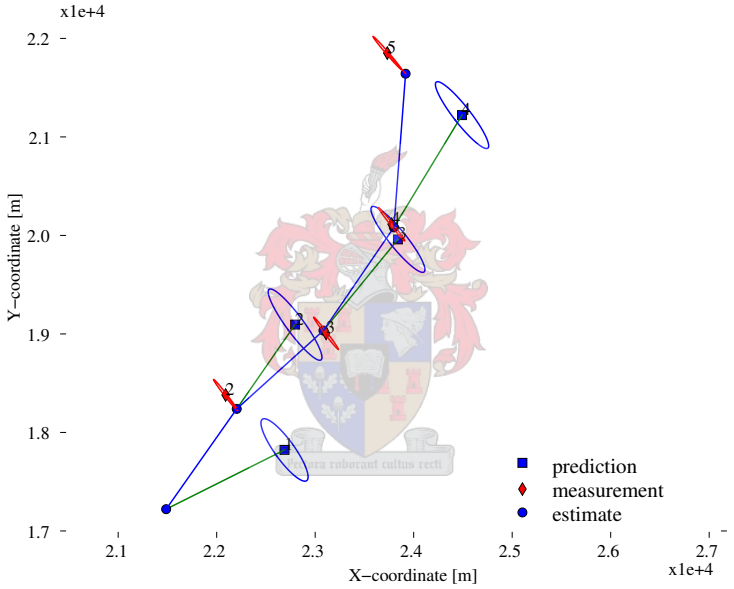

Figure 3.5: Simple filtering illustration

Figure 3.6 illustrates an effect that will become more important in later sections. A 4-state (position and velocity model) Kalman filter attempts to follow a 90° turn, but the predictions take a while to adjust to the new sudden change in velocity. The dynamics of the aircraft therefore manifest in the sense how well a Kalman filter can track certain manoeuvres.

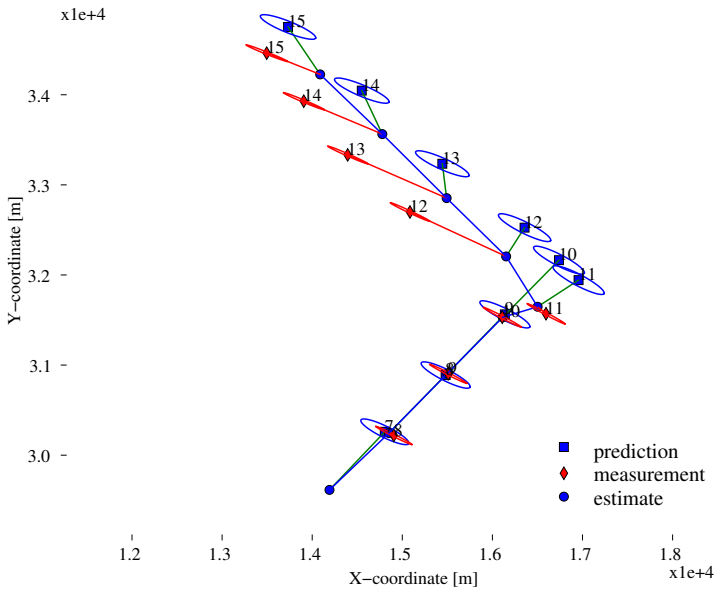

Figure 3.6: Kalman response to an instantaneous turn

3.4 Interacting Multiple Model Filter

It is difficult to choose the correct process noise and model state to describe a specific target. The filter must be capable to track sharp turns, yet remove noise and give a good estimation of the target state for more predictable straight motion. A solution is to follow the multiple model approach by switching between a bank of diverse filters as required.

One kind of multiple model technique switches between different filters according to a certain criteria. Manoeuvre detection by means of doppler radar range rate [10] is useful to detect the start of a high g-turn, indicating that a high manoeuvre Kalman filter can be used. Manoeuvre detection capabilities is not a feature that is always available though.

Another method is the Interacting Multiple Model estimator (as described by [3, p 455]) that mixes the estimates from r Kalman filters according to how well a filter performs. A Markov model describes the transition between the filters, meaning that there are specified probabilities determining how a target will change from one manoeuvre configuration to another.

In this way a low manoeuvre Kalman filter can be used for straight sections, while a high manoeuvre Kalman filter can be used for sections with sudden direction changes. As one performs better, its influence is increased in the mixed output, and similarly decreased as its performance drops.

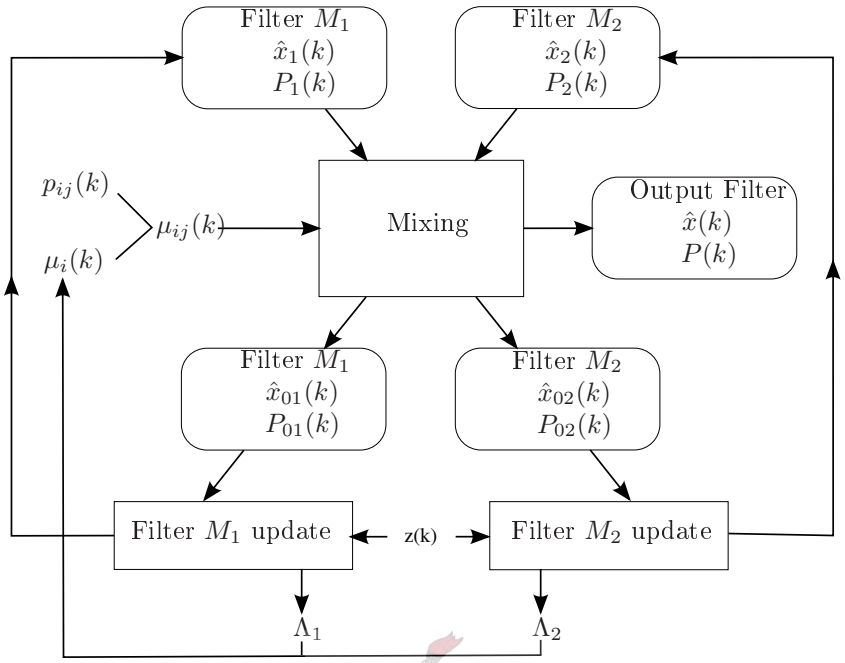

Figure 3.7: IMM diagram

3.4.1 Algorithm

Consider an IMM filter consisting of two filter *modes* as shown in Figure 3.7. Filter M_1 is a low process noise 4-state filter, while M_2 is a high process noise 6-state filter.

The state estimates and covariances are mixed together according to $\mu_{i|j}$, which in turn is a product of the mode probability μ_j and the Markov transition probability p_{ij} between mode i and j. This results in two new filters, with states x_{01} and x_{02} adjusted according to previous performance. Each filter is now updated with measurement $z(k)$, and two new likelihoods $\Lambda_1(k)$ and $\Lambda_2(k)$ are calculated. These are used to calculate new mode probabilities for each filter. This process is then repeated for the next time step.

The output state and covariance of the filter is calculated by mixing the filters together with mode probability μ_j of each filter j.

Calculation of mix probabilities This step calculates the transitional probability $\mu_{i|j}$ that one mode switched to another. The variable $\mu_{i|j}$ expresses the probability that mode M_i was in effect at time $k-1$ given that M_j is in effect at k

$$\begin{aligned}\mu_{i|j}(k-1 \mid k-1) &\triangleq P\{M_i(k-1) \mid M_j(k), Z^{k-1}\} \\ &= \frac{1}{\bar{c}_j} P\{M_j(k) \mid M_i(k-1), Z^{k-1}\} P\{M_i(k-1) \mid Z^{k-1}\}.\end{aligned}$$

The term Z^{k-1} represents the measurement history up to time $k-1$. The switching between modes assumes a Markov process with transition probability

$$p_{ij} \triangleq P\{M(k) = M_j \mid M(k-1) = M_i\}.$$

The term $P\{M_i(k-1) \mid Z^{k-1}\}$ represents the mode probability and is defined as

$$\mu_j(k) \triangleq P\{M_j(k) \mid Z^k\}.$$

Substituting this in the equation we find

$$\mu_{i|j}(k-1 \mid k-1) = \frac{1}{\bar{c}_j} p_{ij} \mu_i(k-1)$$

where the normalizing constant is

$$\bar{c}_j = \sum_{i=1}^{r} p_{ij} \mu_i(k-1).$$

Mixing Each filter calculates a new state by mixing all the filters together according to the mode transition probabilities, where r is the number of modes and $j = 1, ..., r$

$$\hat{x}^{0j}(k-1 \quad | \quad k-1) = \sum_{i=1}^{r} \hat{x}^i(k-1 \mid k-1) \mu_{i|j}(k-1 \mid k-1).$$

The covariance is mixed in a corresponding manner

$$
\begin{aligned}
P^{0j}(k-1 \mid k-1) &= \sum_{i=1}^{r} \mu_{i|j}(k-1 \mid k-1) \\
&\quad \Big\{ P(k-1 \mid k-1) + \left[\hat{x}^{i}(k-1 \mid k-1) - \hat{x}^{0j}(k-1 \mid k-1)\right] \cdot \\
&\quad \left[\hat{x}^{i}(k-1 \mid k-1) - \hat{x}^{0j}(k-1 \mid k-1)\right]' \Big\}.
\end{aligned}
$$

Filter update and likelihood calculation With $\hat{x}^{0j}$ and P^{0j} assigned as mixed states of filter j, measurement $z(k)$ now updates the filter estimates.

The likelihood associated with the filter is calculated from the innovation covariance, and assumed to be Gaussian with mean at the state position estimate

$$
\begin{aligned}
\Lambda_j(k) &= p((z(k) \mid M_j(k), Z^{k-1}) \\
&= N[z(k); \hat{z}^{0j}, S^{0j}].
\end{aligned}
$$

Mode probability calculation Each filter has a mode probability attached, that represents the probability that the current filter is active given the measurement history

$$
\begin{aligned}
\mu_j(k) &= P\{M_j(k) \mid Z^k\} \\
&= \frac{1}{c} p(z(k) \mid M_j(k), Z^{k-1}) P\{M_j(k) \mid Z^{k-1}\} \\
&= \frac{1}{c} \Lambda_j(k) \sum_{i=1}^{r} p_{ij} \mu_i(k-1) \\
&= \frac{1}{c} \Lambda_j(k) \bar{c}_j \qquad \text{with } c = \sum_{j=1}^{r} \Lambda_j(k) \bar{c}_j.
\end{aligned}
$$

The mode probability for time k is calculated using the likelihood derived during the update step, together with the Markov transition probabilities and the mode probabilities from time $k-1$.

Estimate and covariance output The states of each filter remain distinct, and influences each other during the mixing state. An output can be determined at any time by mixing these filters using the mode probability as weight. So it is similar to the mixing step, but this output is not fed back into the algorithmic loop,

$$\hat{x}^j(k \mid k) = \sum_{j=1}^{r} \hat{x}^j(k \mid k)\mu_j(k \mid k)$$

$$P(k \mid k) \quad = \quad \sum_{j=1}^{r} \mu_j(k) \left\{ P^j(k \mid k) + \left[\hat{x}^j(k \mid k) - \hat{x}(k \mid k)\right] \cdot \left[\hat{x}^j(k \mid k) - \hat{x}(k \mid k)\right]' \right\}$$

3.4.2 IMM Example

The following illustrates a simple IMM filter in operation. Two filters form part of the ensemble: one for straight predictable path sections and another for tracking more intensive manoeuvres. The low manoeuvre filter is a 4-state low process noise filter, while the high manoeuvre is handled by a 6-state filter.

For the first track we consider an aircraft flying at an altitude of $4km$, flying north for a stretch and then executing a $2g$ turn before returning south. Figure 3.8 shows the route measurements tracked with predictions and estimates on the left, with the mode probability of the high manoeuvre filter on the right.

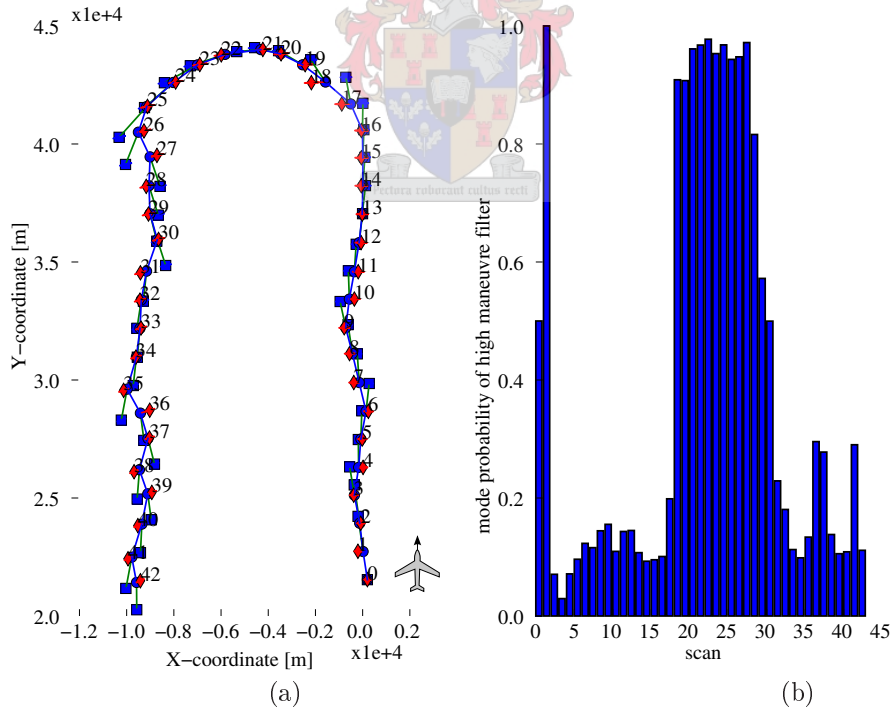

(a) (b)

Figure 3.8: IMM example

a) IMM tracking a $2g$ turn
b) mode probability of the high manoeuvre filter

At the start we see the high manoeuvre filter kicking in strongly. This is an initialisation transient, caused by the high manoeuvre filter capitalizing on the lack of history and resulting uncertainty at the start. The low manoeuvre filter quickly comes into play however, since the long straight section can be predicted accurately. Note that the sum of the mode probabilities sum to 1.0, and since there are only two filters in this scenario, it follows that the low manoeuvre filter mode probability settles around 0.9.

Around scan 15 the turn starts, and the high-filter switches on hard since its higher process noise and additional knowledge of the acceleration state can predict the turning g better.

This lasts until scan 27 whereafter the low-filter returns to dominate for the last straight stretch. Figure 3.9 represents an alternative visualisation of the high filter mode probability. Line lengths represent the mode probability, and their orientation are perpendicular to the estimated velocity.

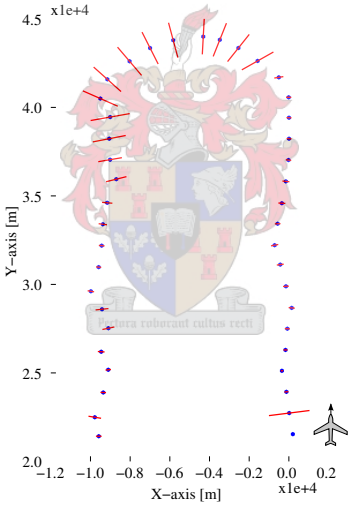

Figure 3.9: Mode probability visualisation of $2g$ turn

An advantage of the IMM is that it mixes between filters that can represent extremes of behaviour. A mix between a low process noise and high process noise filter can effectively give a filter that matches in-between behaviour better than the original filters. This removes some of the importance placed on specifying a correct process noise, since the IMM algorithm will mix an optimal assignment.

Figure 3.10 shows IMM applied on a more complex manoeuvre, consisting of a sequence of $2g$ and $3g$ turns. Note the temporary switch to the low manoeuvre filter at the apogee of each turn.

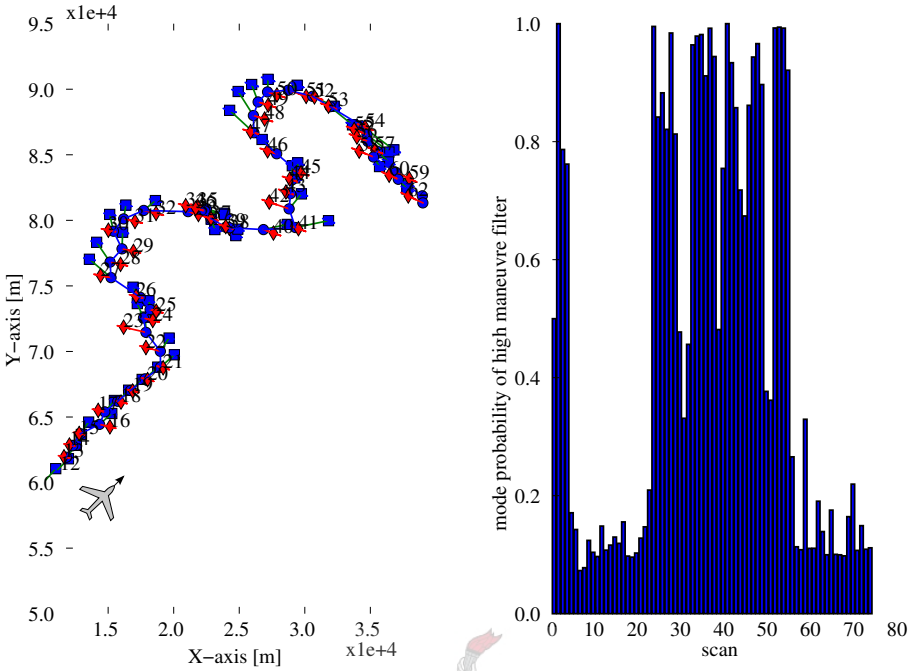

(a) (b)

Figure 3.10: IMM complex example
a) manoeuvre path
b) mode probability of the high manoeuvre filter

3.5 Comparison of filters

The performance of the $\alpha\beta$, Kalman and Multiple Model filters are now evaluated by comparing the root mean square error of the estimated position.

At time step i the root mean square of difference between the true position y_i and the position estimate $\hat{y}_i$ is taken as

$$RMS(\Delta y) = \sqrt{\frac{1}{N}\sum_{i=1}^{N}(y_i - \hat{y}_i)^2}.$$

The error of estimated velocity and heading can be compared as well, but accuracy of position is influenced by all these factors and comparison hence more succinct.

Three different manoeuvres are considered that are representative of aircraft motion as seen in Figure 3.12: A simple straight path, a single $0.5g$ turn and a

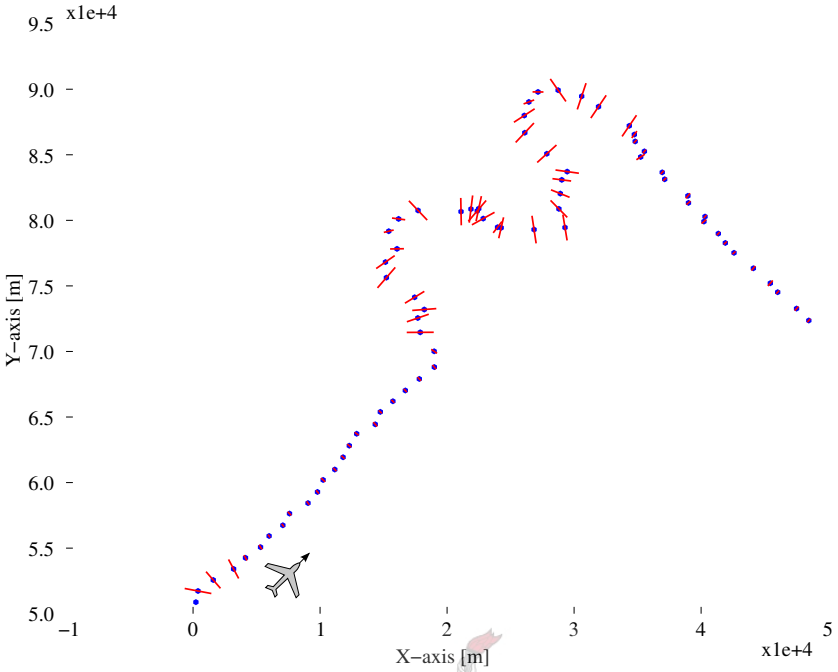

Figure 3.11: Mode probability visualisation of complex manoeuvre

manoeuvre that consists of a combination of sharp g-turns.

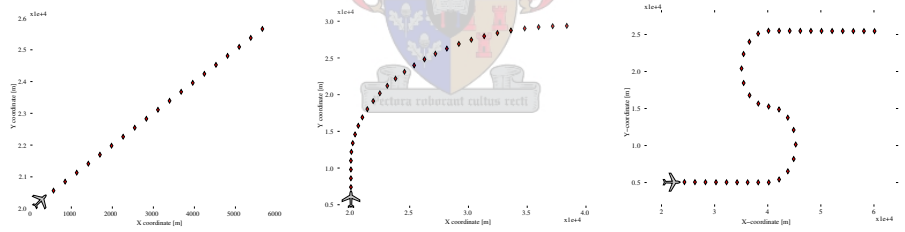

Figure 3.12: Three manoeuvres used in filter the comparison

Each simulation represents 1000 runs of an aircraft flying at a height of 4 kilometres. A radar station is placed by default at the (0, 0) coordinate, and each measurement is simulated appropriately with regards to radar noise and height distortion.

The radar station used corresponds with the characteristics of the Kameelperd radar (Appendix A), therefore no height information is available and each manoeuvre must happen within the $65km$ observation radius.

The filters that will be compared are shown in Table 3.1.

Filter name	Description
AlphaBeta	Reutech filter implementation
Kalman-4L	4 state Kalman, low process noise
Kalman-4H	4 state Kalman, high process noise
Kalman-6L	6 state Kalman, low process noise
Kalman-6H	6 state Kalman, high process noise
IMM	Interactive Multiple Model filter

Table 3.1: Filters used in comparison study

3.5.1 Straight path

The straight path motion involves a simple non-accelerating flight away from the radar station. The initial velocity of $100m.s^{-1}$ is maintained at a height of $4km$.

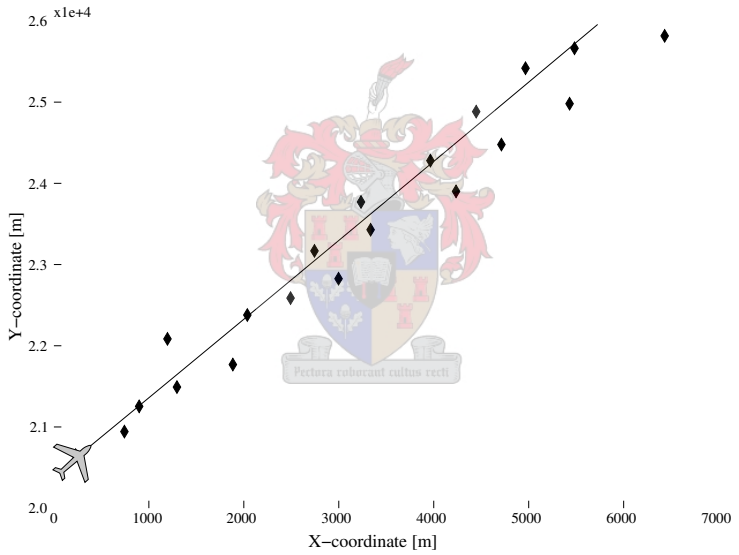

Figure 3.13: Straight path motion

The Alpha-Beta and the low process noise Kalman filter perform the best for this movement. The IMM filter also gives good performance while the high manoeuvre and 6-state filters do not respond so well.

Table 3.2 illustrates the RMS error of each filter together with the percentage that it improves on the RMS error of the raw observation. If it is negative, the observation would indeed be a better choice than the filter estimate for approximating the actual position.

	AlphaBeta	**Kalman4L**	**Kalman4H**	**Kalman6L**	**Kalman6H**	**IMM**
RMS(Δy)	190.006m	183.822m	270.780m	263.692m	286.540m	214.678m
Improving observation	35.00%	37.11%	7.36%	9.79%	1.97%	26.55%

Table 3.2: Straight path results

3.5.2 Single turn

The single turn is a shallow turn of $0.5g$ at a height of $4km$, and is intended to see how filters respond to a slight acceleration.

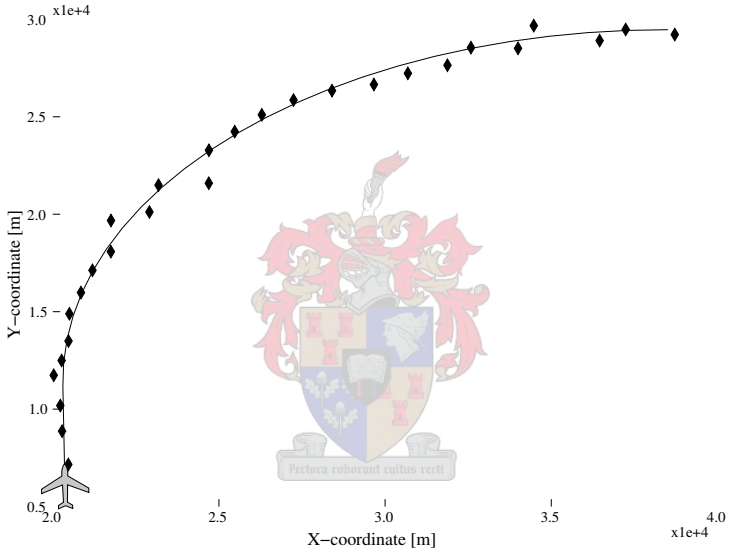

Figure 3.14: Single turn

The IMM filter performs the best with 13% improvement better than the observations.

	AlphaBeta	**Kalman4L**	**Kalman4H**	**Kalman6L**	**Kalman6H**	**IMM**
RMS(Δy)	415.449m	560.755m	395.417m	391.430m	432.726m	376.313m
Improving observation	3.86%	-29.77%	8.49%	9.41%	-0.14%	12.91%

Table 3.3: Single turn results

3.5.3 Combination turn

The combination turn combines two $5g$ turns, and is designed to see how well the filters handle more difficult manoeuvres.

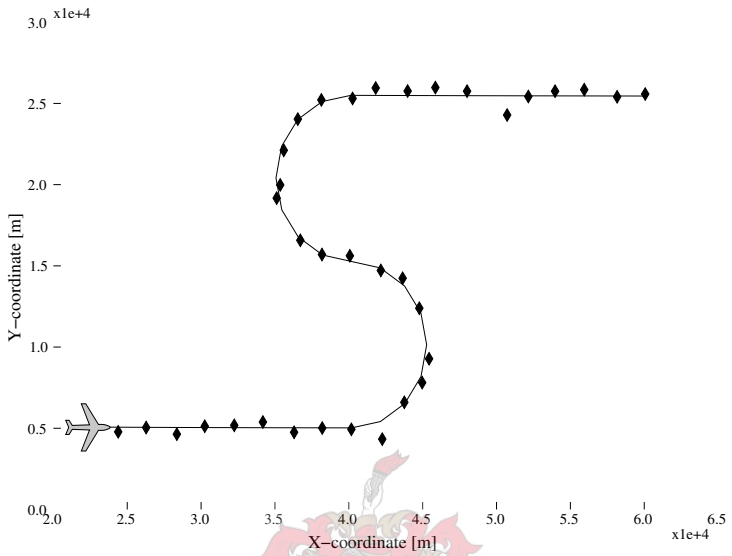

Figure 3.15: Combination turn

Figure 3.15 is an example of a flight configuration that contains straight sections and two tight $5g$ turns. The results are given in Table 3.4, the improvement listed is the percentage it improves from the RMS error of the raw observation. The Kalman 6-state generally performs better on turns, but does not perform well in straight sections. The IMM filter mixes between a low process noise 4-state and a high-process noise 6-state filter, and in this case it performs the best.

	AlphaBeta	**Kalman4L**	**Kalman4H**	**Kalman6L**	**Kalman6H**	**IMM**
RMS(Δy)	689.342m	2401.275m	500.602m	516.678m	535.340m	486.968m
Improving observation	-25.19%	-336.10%	9.09%	6.17%	2.78%	11.56%

Table 3.4: Combination turn results

3.6 Conclusion

By using an estimation filter to model an aircraft, the noisy nature of the measurements are minimized and we can estimate an aircraft's current position and future state.

The number and nature of the states that are described by the dynamic model and the choice of the coordinate system can vary extensively. There is difficulty in choosing correct parameters to describe the motion of something as unpredictable as an aircraft, but by using a combination of complementing filters a multiple model approach offers a good solution. A multiple model filter also adapts to the nature of a manoeuvre, and is thus more robust to different changing scenarios.

Equipped with the modeling tools to track a single aircraft, we now investigate the tracking of multiple targets.

Chapter 4

Track Management

4.1 Introduction

A Kalman filter is a good device to estimate and predict the position of an aircraft. This would be sufficient for the tracking of a single object under ideal conditions, but the reality of the situation is more complex.

In cases where multiple aircraft fly in paths that interact closely, the noisy nature of the measurements can make the association of the measurements with the correct tracks hard. This is made even more difficult when considering the additional challenges faced by a radar system:

- False reports: Radar clutter noise causes false detections.
- Missing reports: Some targets not detected during a scan.
- New targets: As some targets enter the search volume, their appearance should be noted.
- End of targets: Targets can move out of the search volume.

While a simple Kalman filter is enough for the tracking of a single aircraft, more logic is required when multiple targets are introduced in an already noisy system.

Figure 4.1 demonstrates how a simple straight flight configuration of three aircraft can be confused by a tracker. In this example, one measurement during scan 1 is considered a false target, while a measurement from scan 2 is considered the start of a new track. With missed detections included, it is even more difficult for a radar system to give an accurate picture of what is happening in the air.

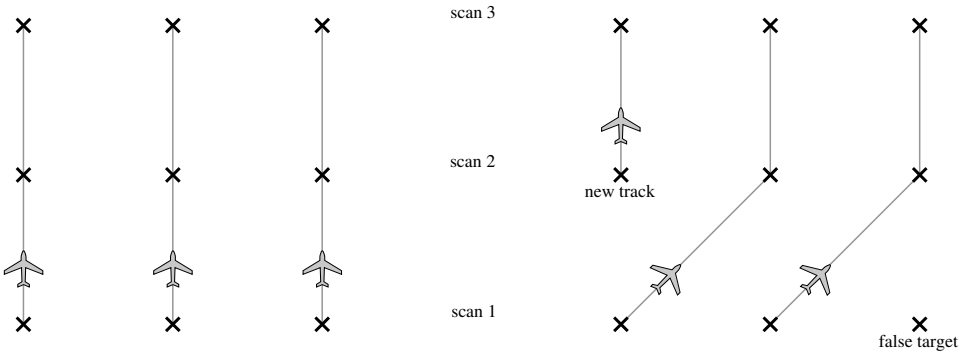

Figure 4.1: Flight of three aircraft with wrongly tracked interpretation.

4.2 Multi-target techniques

There are various methods to handle the tracking of multiple targets, ranging from simple to more complicated. The following sections give an overview of the more popular techniques in use today.

4.2.1 Global Nearest Neighbour (GNN)

In the Nearest Neighbour system the best measurement association is made after each scan. A Kalman filter or other predictive device is assigned to each track and makes a prediction of the target's future position. The measurement closest to the prediction is assigned to that track. This is the naive implementation, but assignments can also be made based on a strategy to minimize the global summed distance function of all tracks.

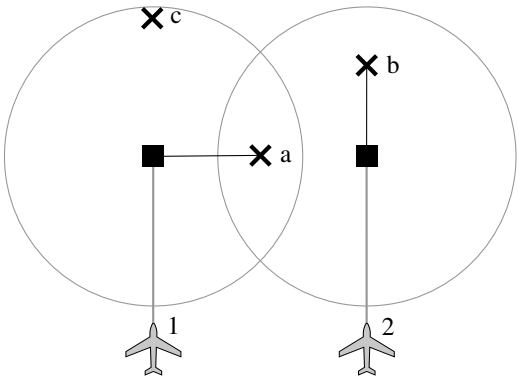

Figure 4.2: Global Nearest Neighbour data association.

This is illustrated in Figure 4.2, where aircraft 1 and aircraft 2 have predicted

positions indicated by squares. Measurements are gated around the prediction, so that only measurements within a certain distance range are taken under consideration for each aircraft.

In this situation measurement a falls in the range of both predictions, and is an equal distance away from each. In this case the assignment of measurement a to aircraft 1 and measurement b to aircraft 2 minimizes the summed distances of both tracks. Measurement c is therefore considered a false detection.

Nearest neighbour is a simple algorithm, but it only performs well in low noise environments with targets remaining widely spaced. There are more advanced algorithms that are better at handling noisy high-traffic radar environment.

4.2.2 Joint Probabilistic Data Association (JPDA)

Probabilistic Data Association (PDA) is an algorithm created by Bar-Shalom and Tse [4], where every track is updated by a weighted sum of all observations within the gating distance. Each track is represented by a Kalman filter.

The PDA works well in a single target environment, but for multiple targets the algorithm was extendedinto the Joint Probabilistic Data Association (JPDA). In JPDA the weight of the measurements that are shared by the gates of the tracks are diminished. In the case of Figure 4.2, the effect of measurement a would be reduced since it falls in the range of both tracks.

The creation of new tracks is not handled by the algorithm, so an additional track initiating system is needed. The algorithm is *target-oriented*, so a measurement is considered with respect to established targets.

4.2.3 Multiple Hypothesis Tracker (MHT)

The Multiple Hypothesis Tracker considers every possibility of data association, and generates a probability for each of these hypotheses. The hypotheses are propagated into the future, deferring hard decisions until later. This causes an explosion of possibilities as every hypothesis gives rise to many more. Attention must thus be given to cull less likely hypotheses, so that the calculations remain managable.

Figure 4.3 depicts the parallel flight of two aircraft for the duration of 3 radar scans. Each scan yields two measurements. Under ideal circumstances there are two hypotheses after two scans, and four hypotheses after three scans as shown in the figure. At the end of three scans, Hypothesis 0 is the most likely with

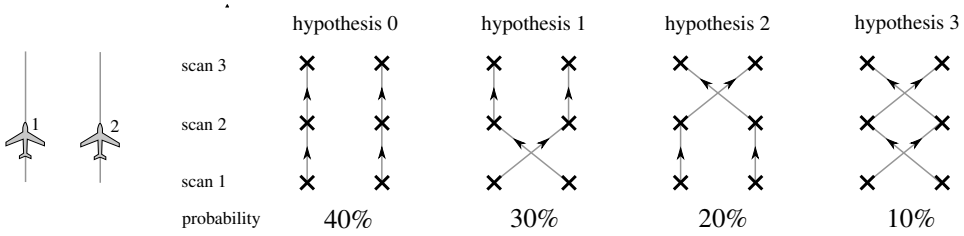

Figure 4.3: Four typical hypotheses in a MHT system with probabilities.

a probability of 40%, while the more unlikely Hypothesis 3 is a candidate for removal.

The tracker considers Hypothesis 0 the most likely, but it is important to realize that this ranking is not set in stone. Each track in a hypothesis is described by a Kalman filter, and produces a track prediction accordingly. The set of measurements from the next scan might fit the predictions from Hypothesis 1 better, increasingly its likelihood. Thus decisions are deferred until more information becomes available.

Given infinite computational powers, MHT gives the answer to the optimal estimation association problem. Such exhaustive analysis is of course not practical, and the hypotheses need to be culled. Yet MHT still performs better than JPDA solutions in general [9]. The fact that MHT includes track initiation as part of the algorithm is also an advantage, in contrast with PDA that needs additional rules for creating new tracks.

The MHT algorithm is a method that seems most promising for Identity Confidence calculation. It is measurement-oriented, and therefore attaches more value on the measurements than on the already established targets. The history of a situation plays a greater role than in other tracking algorithms, and this gives a hint that it is useful in performing identity analyses.

4.3 MHT System

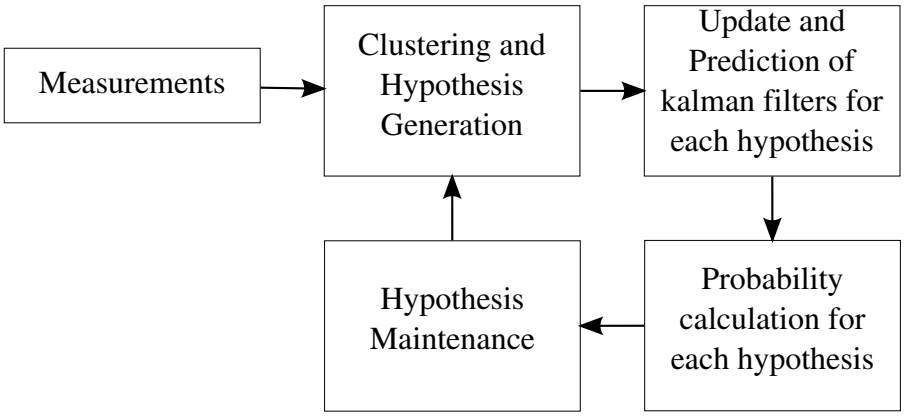

Figure 4.4: Elements in a MHT system

The Multiple Hypothesis system manages a collection of hypotheses, each hypothesis representing a situation of possible targets and paths that could have been followed. So each hypothesis consists of a collection of tracks, where a track is a sequence of measurements and missed detections that represent the possible movement of an aircraft.

For the measurements from each scan the MHT looks at each of the existing hypotheses and creates new hypotheses for every possibility of track-measurement association. Missed detections, false targets and new targets are handled as well. Since this involves a lot of possibilities, the measurement is gated so that it is only considered for association if it falls within the gating window of a track.

The next step is to estimate and predict the tracks. Each track of a hypothesis is represented by a Kalman filter, and each one is updated according to the previously associated measurement.

Now the probability of a hypothesis is updated according to the measurement association and its nature. After this the hypotheses are compared, and those that are less likely are removed. At this moment the system awaits the next batch of measurements to restart the cycle.

4.4 MHT Theory

Following Blackman [5] the probability of a data association hypothesis after K scans is described by

$$Q_K = P_0(n_K, n_{FK}) \prod_{i=1}^{n_K} \left[P_{TL}(D_i) P_{DT_i}(NU_i|D_i) \prod_{i=1}^{NU_i} P_{ER}(\tilde{y_{il}}) \right]. \tag{4.1}$$

The equation consists out of the following elements:

- **Sources**: $P_0(n_K, n_{FK})$ is the probability associated with choice of n_{FK} false targets and n_K true targets
- **Deterioration**: $P_{TL}(D_i)$ is the probability of track length D_i
- **Detection**: $P_{DT}(NU_i|D_i)$ is the probability that track i produces NU_i detections given that the track length is D_i
- **Association**: $P_{ER}(\epsilon_{il})$ is the probability of residual error for lth observation included in the ith track

The *sources* term is influenced by the number of targets present in the hypothesis. The *deterioration* and *detection* terms are considered for each track in the hypothesis, while the *association* term is computed for each measurement of each track.

4.4.1 Sources

> $P_0(n_K, n_{FK})$ is the probability associated with choice of n_{FK} false targets and n_K true targets.

The sources term describes the probability that in this hypothesis a specified number of false targets and new targets have *entered* the search volume, and is given by

$$P_0(n_K, n_{FK}) = P_{0F}(n_{FK}) P_{0T}(n_K),$$

where $P_{0F}(n_{FK})$ is the probability of n_{FK} false targets and $P_{0T}(n_K)$ the probability of n_K true targets.

In the case of the false target, the assumption is made that false targets occur randomly in space during each scan with a uniform probability density β_{FT}. For a small volume Δ the probability of a false target is therefore $\beta_{FT}\Delta$. First we consider a single scan k with n_{Fk} false targets

$$P_{0F}(n_{Fk}) = (\beta_{FT}\Delta)^{n_{Fk}} (1 - \beta_{FT}\Delta)^{N_C - n_{Fk}},$$

where $N_C = V/\Delta$ is the total number of cells. Further with the assumption that $N_C \gg n_{Fk}$,

$$(1 - \beta_{FT}\Delta)^{N_C - n_{Fk}} \approx (1 - \beta_{FT}\Delta)^{N_C} = (1 - \beta_{FT}\Delta)^{V/\Delta}$$

and for a small cell size Δ

$$\begin{aligned} \lim_{\Delta \to 0} (1 - \beta_{FT}\Delta)^{\frac{V}{\Delta}} &= \lim_{\Delta \to 0} \mathrm{e}^{\frac{V}{\Delta} \ln(1 - \beta_{FT}\Delta)} \\ &= \lim_{\Delta \to 0} \mathrm{e}^{\frac{V}{\Delta}(-\beta_{FT}\Delta)} \\ &= \mathrm{e}^{-\beta_{FT}V}. \end{aligned}$$

Thus the probability of false targets during scan k is

$$P_{0F}(n_{Fk}) = (\beta_{FT}\Delta)^{n_{Fk}} \mathrm{e}^{-\beta_{FT}V},$$

and similarly for new targets,

$$P_{0T}(n_k) = (\beta_{NT}\Delta)^{n_k} \mathrm{e}^{(-\beta_{NT}V)}.$$

The combination of K scans of false targets involves taking the product of the scan probabilities

$$\begin{aligned} P_0(n_K, n_{FK}) &= \prod_{k=1}^{K} P_0(n_k, n_{Fk}) \\ &= \prod_{k=1}^{K} P_{0F}(n_{Fk}) P_{0T}(n_k) \\ &= (\beta_{FT}\Delta)^{n_{FK}} (\beta_{NT}\Delta)^{n_K} e^{-\beta KV}, \end{aligned}$$

where $\beta = \beta_{FT} + \beta_{NT}$.

Reid [16] includes the probability of the possible assignment given the specific configuration of false, prior and new targets. The final equation is similar to that of Blackman [5] after simplification and constant combination.

4.4.2 Deterioration

$P_{TL}(D_i)$ is the probability of track length D_i.

The track length term is useful to describe the likelihood of a track disappearing from the search volume. This could possibly be based on the position of the aircraft in the search volume, or taking into account geographical features. Sittler [17] makes an assumption that the target length density function can be approximated by the exponential distribution as in Equation 4.2, showing that it matches experimental ship tracking data closely. In this case it is applied on aircraft movement.

$$f(\tau) = \frac{\mathrm{e}^{-\tau/\tau_0}}{\tau_0} \tag{4.2}$$

The probability of the track terminating in one the interval D_iT to $(D_i + 1)T$, where T is the sampling time and D_E is the expected track length expressed as the number of scans, is given by

$$P_{TL1}(D_i) = \frac{1}{\tau_0}\int_{D_iT}^{(D_i+1)T} \mathrm{e}^{-\tau/\tau_0} d\tau = (1 - \mathrm{e}^{-1/D_E})\mathrm{e}^{-D_i/D_E}. \tag{4.3}$$

The probability that the track did not terminate and has a track length greater than D_i is given by

$$P_{TL2}(D_i) = \frac{1}{\tau_0}\int_{D_iT}^{\infty} \mathrm{e}^{-\tau/\tau_0} d\tau = \mathrm{e}^{-D_i/D_E}. \tag{4.4}$$

So depending on whether a measurement is registered for a track during a scan,

$$P_{TL}(D_i) = \begin{cases} P_{TL1}(D_i), \text{ measurement not registered} \\ P_{TL2}(D_i), \text{ measurement registered} \end{cases}.$$

4.4.3 Detection

> $P_{DT_i}(NU_i|D_i)$ is the probability that track i produces NU_i detections given that the track length is D_i.

After each scan a track is either updated with a measurement or the detection is consider missed. P_D is the probability of detection, and is a value typical to a specific radar system. The detection term gives the probability of a certain detection history for a track. In the case of NU_i detections and $D_i - NU_i$ misses,

$$P_{DT} = P_D^{NU_i}(1 - P_D)^{(D_i - NU_i)}.$$

4.4.4 Association

> $P_{ER}(\epsilon_{il})$ is the probability of residual error for lth observation included in the ith track.

The main contribution to the probability of a hypothesis is to what extent the measurements are successfully associated to tracks. Finding this probability we use a multivariate Gaussian distribution to describe the probability density function of the residual error (the difference between the predicted and the real measurements).

The innovation covariance S and the measurement prediction $\hat{z}$ of the track's Kalman filter is used, see Kalman filter Equations 3.5 and 3.6

$$\begin{aligned} S &= HPH^T + R_c \\ \hat{z}(k \mid k-1) &= H\hat{x}(k \mid k-1) \\ \epsilon(k) &= z(k) - \hat{z}(k \mid k-1). \end{aligned}$$

The density function is evaluated with the measurement as input

$$f(\epsilon) = N[z(k); \epsilon(k|k-1), S] = \frac{\mathrm{e}^{-\epsilon^T S^{-1} \epsilon/2}}{(2\pi)^{D/2}\sqrt{|S|}},$$

where D is the dimension of the measurement. The pdf is converted to a probability by multiplying it with the infinitesimal cell volume Δ. The association error probability for a track is computed by combining the probabilities for each measurement-prediction association. Let ϵ_{il} represent the innovation error of the lth measurement with respect to the ith track

$$P_{ER_i} = \Delta^{NU_i} \prod_{l=1}^{NU_i} f(\epsilon_{il}).$$

The association error probability for a hypothesis is computed by combining the probabilities for every track

$$P_{ER_i} = \Delta^{NU_i} \prod_{i=1}^{n_K} \prod_{l=1}^{NU_i} f(z_i(l)).$$

4.4.5 Combined Expression

Combining the expressions given above,

$$Q_K = C\beta_{FT}^{n_{FK}}\beta_{NT}^{n_K}\prod_{i=1}^{n_K}\left[P_{TL}(D_i)P_D^{NU_i}(1-P_D)^{D_i-NU_i}\prod_{j=1}^{NU_i}f(z_j(l))\right]. \quad (4.5)$$

The constants have all been combined into a single term $C = \Delta^{n_K+n_{FK}}e^{-K\beta V}$. The cell and scan volume remain the same across hypotheses, and does not play a role in the comparison of probabilities.

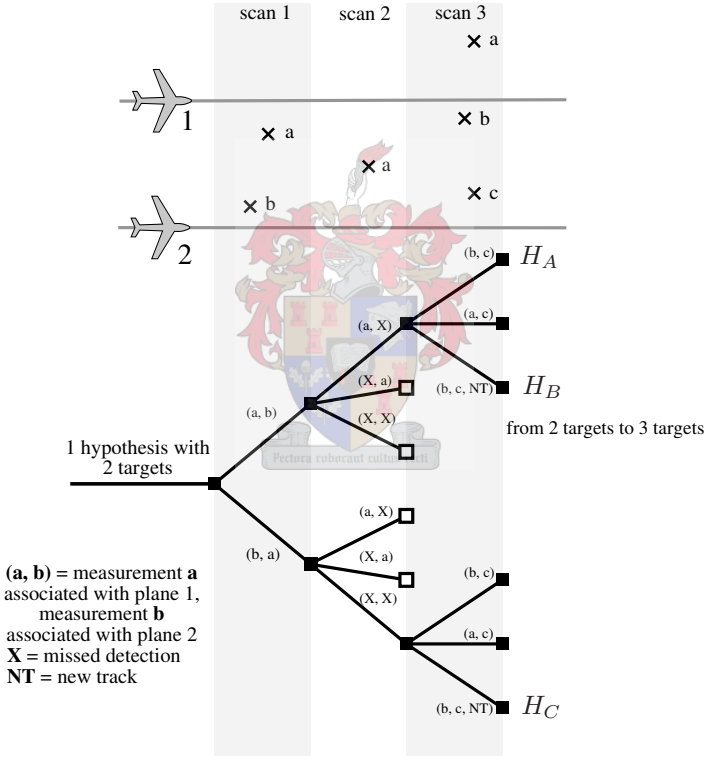

Figure 4.5: Hypothesis branching over time

$$\begin{aligned} P(H_A) &= \beta_{nt}\beta_{ft}P_D^5(1-P_D)\prod g_{A1..A5} \\ P(H_B) &= \beta_{nt}^2P_D^5(1-P_D)\prod g_{B1..B5} \\ P(H_C) &= \beta_{nt}^2\beta_fP_D^4(1-P_D)^2\prod g_{C1..C4} \end{aligned} \quad (4.6)$$

Figure 4.5 illustrates the tracking of the flight of two aircraft over three sets of measurements and (4.6) gives the resulting probabilities. A single hypothesis at the start represents two aircraft tracks, and at each scan the hypothesis is branched into new hypotheses. In the figure, a branching tuple (a, b) indicates that measurement a of the current scan is assigned to the track of aircraft 1 and measurement b assigned to the track of aircraft 2. The term g_{A1} represents the association probability of H_A during scan 1. H_A considers observation a of scan 3 correctly as a false target, while H_B and H_C consider it the start of a new target. During scan 2 there is only one observation - so a target has been missed. H_C considers that single observation as a false target.

Figure 4.5 is a relatively simple example, and the full hypothesis tree generated is substantially more involved than the one depicted here. Culling is therefore essential to prevent an unmanageable number of hypotheses as demonstrated at the end of scan 2.

4.4.6 Adjusting for miscorrelation

The Kalman filter can have a very optimistic process covariance. Miscorrelation however represents a source of error that should be included. This is especially important with MHT since the innovation covariance of the Kalman filter is used to calculate probabilities.

Miscorrelation means that when two tracks move close to one another the possibility of incorrect data association needs to be reflected. In essence this means that the process covariance is increased.

Define a variable γ to represent a correct data association. If $\gamma = 1$ the observation associated successfully, and if $\gamma = 0$ the observation is either a false target or from another track. The Kalman filter equations (3.7) - (3.8) are now adjusted to include

$$\begin{aligned} \hat{x}(k \mid k, \gamma) &= \hat{x}(k \mid k-1) + \gamma K(k)\epsilon(k) \\ P(k \mid k, \gamma) &= (I - \gamma K(k)H)P(k \mid k-1). \end{aligned}$$

When γ is equal to 0 the situation is similar to when no association happened and the straight predictions are taken as the new estimates. The probability of correct correlation $P_{CC} \triangleq p(\gamma = 1)$ is now used to mix the $\gamma = 1$ estimate with the $\gamma = 0$ estimate.

Finding the value of P_{CC} in the following equation is the only remaining challenge,

$$\begin{aligned}\hat{x}(k \mid k) &= P_{CC}\hat{x}(k \mid \gamma = 1) + (1 - P_{CC})\hat{x}(k \mid k, \gamma = 0) \\ P(k \mid k) &= \sum_{\gamma=0}^{1} p(\gamma)[P(k \mid k, \gamma) + \hat{x}(k \mid k, \gamma)\hat{x}^T(k \mid k, \gamma)] - \hat{x}(k \mid k)\hat{x}^T(k \mid k).\end{aligned}$$

In this case we have assumed a fix value for our simple case of interacting aircraft, but one can determine it more accurately during the MHT association process [5, p 105].

4.5 Variations in implementation

4.5.1 Data representation

There are many variations in how hypotheses can be represented computationally. The method of Reid [16] uses static matrix structures that are expanded as new observations are encountered.

With the advent of modern computer languages dynamic data structures seems more promising, offering easier implementation and possibilities of data reuse. Tracks that are shared between hypotheses can be represented by a single data structure. This is how it is implemented in this thesis.

4.5.2 Pruning

A disadvantage of considering every possibility in systems like MHT, is that hypothesis growth is exponential. An important part of the system is therefore to select the possiblities that are more likely, and to discard unlikely ones so that hypothesis growth is kept in check. There are many variations how unlikely hypotheses can be discarded or combined.

It is important that the pruned hypothesis tree still be representative of reality. This is something that we will consider in more detail later.

Threshold

One method is to discard all hypotheses with probability below a fixed threshold. A disadvantage of this is that it does not take into account the computational

resources available. For example, it may lead to the removal of more hypotheses than is necessary. Likewise it can lead to the removal of too many hypotheses if most of them fall below the threshold.

N-scan

Another method is the N-scan algorithm that unites all hypotheses with the last N measurements in common. In other words, a sliding window is applied to combine hypotheses that have tracks that are nearly similar. Restricting the algorithm to zero-scan, one can find a similarity with the PDA [16] which combines all the hypotheses into a single one after each step.

Fixed breadth

The scan breadth approach restricts the hypotheses to a fixed number. The best N hypotheses are therefore selected and the rest discarded. A disadvantage is that it can take some processing time to find the best hypotheses after each time step. This method is the easiest to implement though and keeps the amount of computation consistent.

Since MHT can be described as a Maximum A Posterior (MAP) estimation, another method is to use the Viterbi algorithm [7] to select the most probable hypotheses.

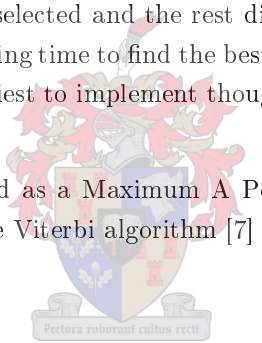

N-scan track based

Blackman [6] describes a method that implements pruning by altering the way we consider hypotheses. Instead of working with hypotheses Blackman suggests we operate on the tracks as fundamental unit as depicted in Figure 4.6.

Each time a choice is offered for a track between two observations, the track is split into two tracks. These tracks are kept in a *family,* that is represented by a tree structure keeping track of a track's lineage.

A hypothesis is now constructed by picking a track from each family. Only one track in a family can belong to a hypothesis since none of the tracks in a hypothesis may share a measurement. Not all tracks from every family are compatible, so all working combinations must be found. Hypotheses are thus reconstructed from scratch out of the track families after each scan.

Figure 4.7 shows how culling works by selecting the best hypothesis, and for each track finding the track's ancestor N scans into the past. This node is now

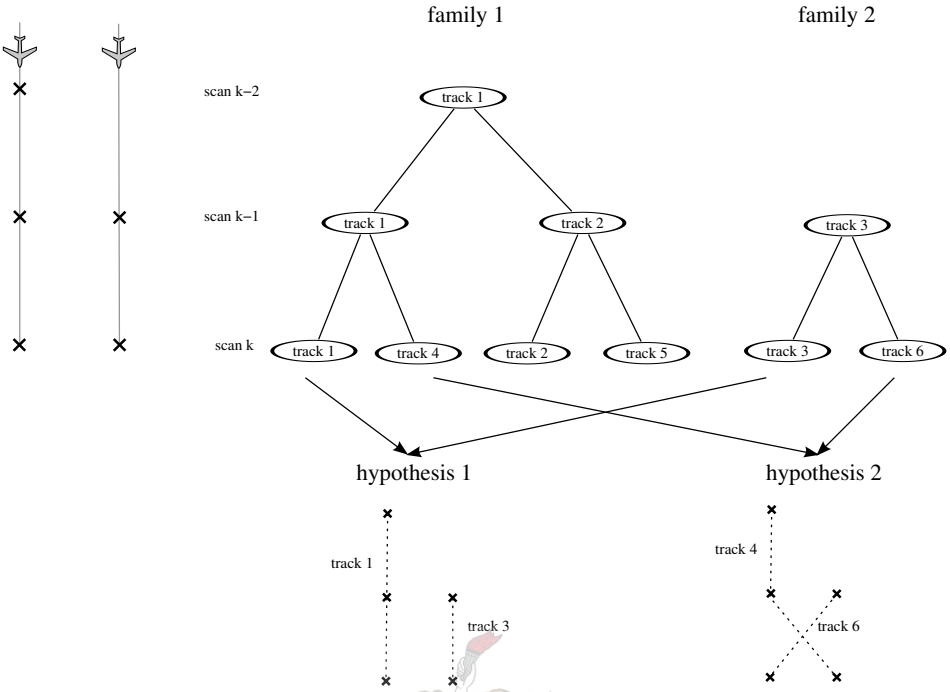

Figure 4.6: Track-based MHT

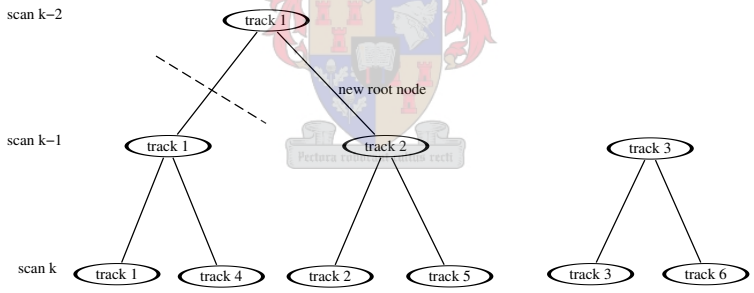

Figure 4.7: Track-based culling for $N = 2$

considered the root node of a family and the tracks that are not its children are discarded.

4.5.3 Clustering

The nature of MHT is such that the normal gating procedure does not play a large role in data association process. Since the unlikely possibilities are immediately culled, the MHT itself serves a function as a gate. Considering unlikely associations is a waste of processing so the problem is often split into smaller ones. This is known as *clustering*. When the radar detects an aircraft

far removed from the other it can be considered in isolation. It is only when aircraft approach in close proximity that their fates become intertwined.

4.5.4 Choice of filter

A Kalman filter describes and predicts the movement of an aircraft, and as seen in Section 3.5, certain Kalman filters specialize in handling certain kinds of manoeuvrability better than others. There are two strategies to use multiple models as part of a multiple hypothesis tracker. One way is to create separate hypotheses to handle high and low manoeuvres, but aircraft manoeuvrability is rarely an either-or case. A better way is the use of the Interacting Multiple Model technique that aims for the best of both worlds.

Chapter 5

Identity Confidence

5.1 MHT as analysis tool

A tracker outputs a series of tracks each consisting of a set of associated measurements, while the other remaining measurements are considered false targets. The task of identity confidence estimation is to take a track, and by comparison with the measurements, determine the probability that its identity integrity remained preserved. In essence, what is the chance that the target moved from the starting point to the end of the track.

The idea is to use the MHT algorithm retrospectively and consider all the other likely possibilities. Given the initial tracks and their endings, the MHT can reconstruct possible tracks and combine the probability of all scenarios with a specific track start and ending in common. This is similar to using a MHT as a tracker, but differs by giving initial tracks as input.

The idea of this system is to serve as a support system for radar operators. While it is essential for tracking systems to operate in real-time, a system such as this can be applied at a problem area after the fact and is expected to give an answer within a reasonable amount of time. This algorithm can therefore be more complex and be simulated at greater depth than a normal tracking algorithm.

5.2 Algorithm

Given a specific track, the goal is to find an estimate of the probability that the target did indeed move from the beginning to the end. The assumption

is made that the aircraft in question do in fact exist, so the starting points of the tracks supplied by the tracker are taken as known. The MHT algorithm is initialised with these track starting points and is run on the subsequently received measurement data.

The MHT constructs all the possible hypotheses of target movement, and assigns a probability to each. Finding the identity confidence of the initial track involves the combination of all the probabilities of the hypotheses that match it. A hypothesis matches the initial track when it contains a track that matches the start and end point. In essence, the hypotheses with all the different possible variations of the track movement are compared with hypotheses where the track movement do not occur. Where $H[tracks]$ select the hypotheses containing any of the supplied tracks, and $track[z_a, z_b]$ selects the tracks starting with z_a and ending with z_b,

$$P(z_a \rightarrow z_b) = \sum P(H[track[z_a, z_b]])$$

gives the probability that an aircraft moved from starting observation z_a to the suspected end observation z_b.

5.3 Implementation

Since multiple hypothesis tracking inherently involves dynamic tree-like data structures, it is prudent to use a programming language that allows dynamic datastructures.

For this project Python was chosen as the language of implementation, since it handles dynamic structures while providing a system that invites experimentation. Its major disadvantage is execution speed which is important for MHT in practise. Optimizing the Python code by implementing performance intensive sections in C could solve these issues, but for an experimental prototype the current system is adequate.

There are a few components involved in the system design as seen in Figure 5.1. Appendix (B) elaborates on the software system in greater details.

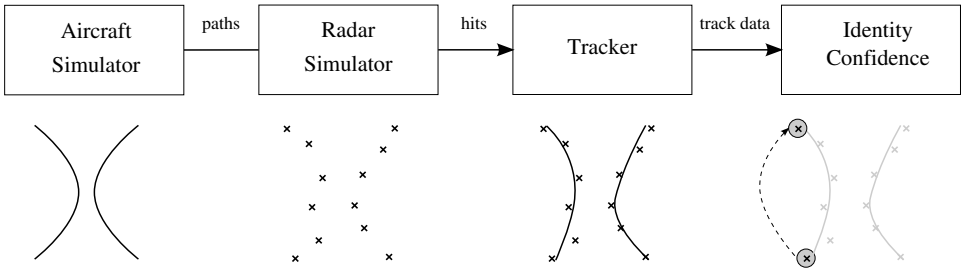

Figure 5.1: System components and illustrations of the function of each.

The foundation of the system is an aircraft track and radar simulator that gives realistic measurement observations. The observations are sent to a tracker and a pair of most likely tracks as output. Now the identity confidence algorithm runs on a track and estimates the probability that the supposed track movement actually happened.

5.3.1 Aircraft simulator

The module simulates one or more aircraft to make turns of a certain g, or to fly straight in a specific bearing for a set amount of time. It was used in calculating typical process noise covariances and for simulating the aircraft in each scenario.

5.3.2 Radar simulator

The simulator makes observations from the simulated paths corrupted by noise as specified of a radar from the industry. The specifications for the radar used are listed in Appendix A. The radar simulator is capable of missing detections and making false detections according to specification, but although the developed tracker can handle this it was not the focus of this project.

The radar receives the paths generated by the aircraft simulator and adds stochastic noise to give discreet *hit* events that represent the observation of the aircraft as it is detected by the radar beam.

5.3.3 Tracker

The system needs a tracker to process the observations. The tracker used is a Multiple Hypothesis Tracker with culling restricting the hypotheses with the fixed breadth method to around 20 - 50. For our limited situation this is sufficient but other MHT systems often go as deep as 200.

5.3.4 Identity Confidence

The Identity Confidence algorithm calculates the identity probability of a target track in the context of the other observations. It receives a track from the tracker, and then it analyzes what the probability is that a target moved from the starting point to the end point.

5.4 Effect of manoeuvre orientation

It is not possible to resolve two aircraft flying in parallel formation for an extended length of time. The confidence in the identity is expected to be 50%, implying that the real identity of the end result of a track is completely uncertain.

The proximity of the tracks and the detail of the manoeuvre largely determine the identity confidence. Shallow turns and crossing of tracks are an obvious indication of easily confused tracks. Another factor is the position and orientation of the radar site with regard to the interaction zone. The noise covariance of the radar is typically an elongated ellipse, so close manoeuvres in certain directions should cause greater confusion, as illustrated in Figure 5.2 *a* and *b*. This is simulated in Section 5.6.2.

Noise is probabilistic - so it is possible for closely moving aircraft to retain some identity after an interaction, if noise distorts the path fortuitously as seen in Figure 5.2 *c*. All these factors are handled well by the MHT, and explains some of the variation obtained in the results.

5.5 Approximation caused by culling

Using the MHT as a tracker and using it to analyse a scenario differs subtly. The culling of hypotheses is essential to MHT operation, so it is a given that the MHT describes an approximation to the problem.

When applied to identity confidence the MHT needs to keep accurate track of all possibilities. As certain hypotheses dominate it will do so with some margin of error. On the other hand, if the hypotheses are of all equal likelihood hypothesis culling may dramatically influence the results. Culling unlikely hypotheses can bias a situation much more than when using MHT as a tracker, and when analysing a situation this must be handled with care to give an accurate representation of the situation.

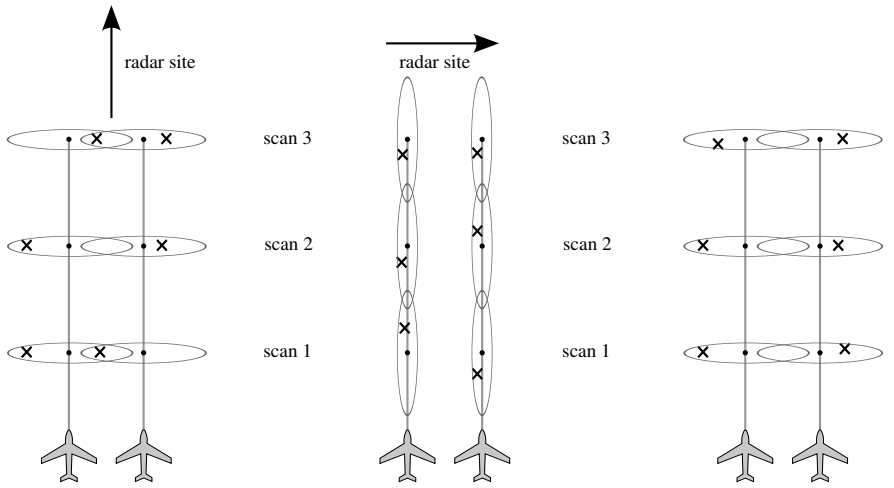

a) Possible track confusion as noise covariances overlap

b) Track integrity preserved as noise covariances distinct

c) Noise covariances overlapping, but with fortunate measurement allocation

Figure 5.2: Probabilistic noise influences on identity

It is therefore essential that the probabilities of the deleted hypotheses be re-distributed over the remaining hypotheses. This is done by merging the deleted hypothesis probabilities with other hypotheses that represent the same outcome. In other words hypotheses where the tracks have the same beginning and endings.

5.6 Simulations

5.6.1 Crossing flight pattern

The simplest case of interacting aircraft is a crossing bypass flight. Two aircraft flying close to each other in the same direction offers no chance of track identity preservation. On the other hand, flying past each other in opposite directions no confusion should be possible.

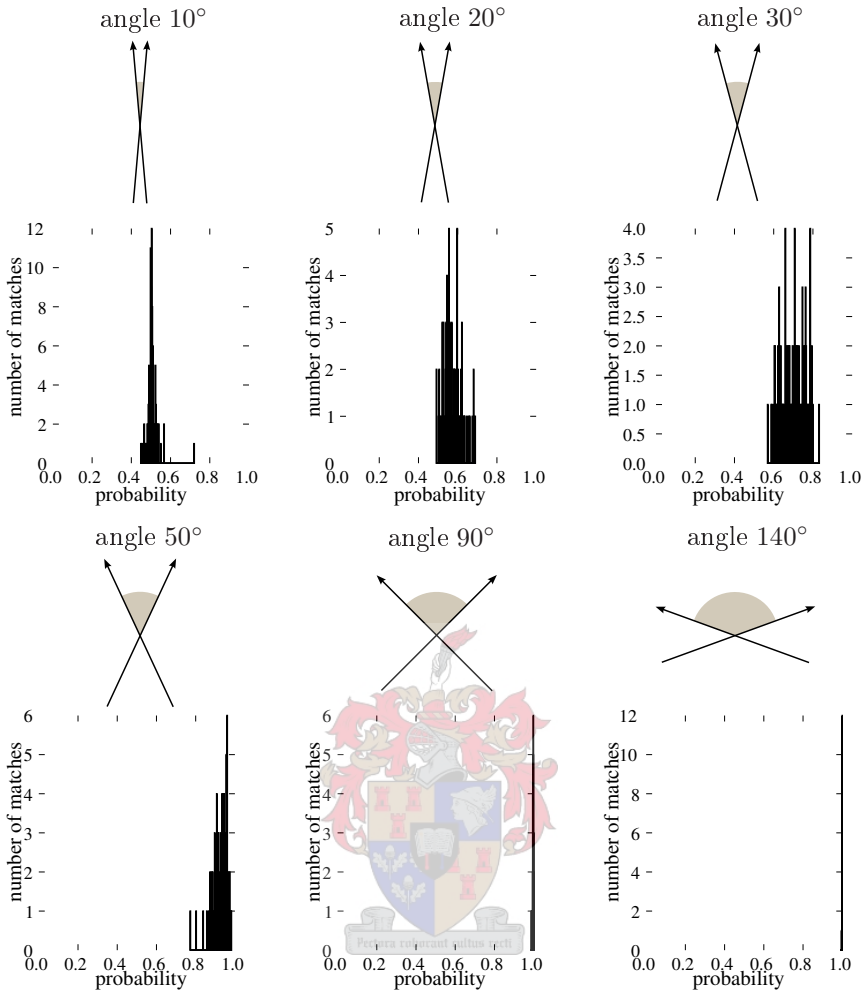

Figure 5.3: Identity confidence of crossing flight patterns

Figure 5.3 shows results of different bypass configurations for 100 runs each expressed in histogram format. The probability considered is the probability that the aircraft flight paths did indeed cross. With 10 degree crossing the choice between the two possibilities (as shown in Figure 1.1) is equally likely, while at 140 degrees confusion is considered unlikely. These results confirm intuition.

For the lower intersection angles, there is a slight negative deviation from the expected 50 percent that is probably due to too many nearly equal hypotheses being culled. As discussed in Section 5.5 a situation with many hypotheses of equal probability cannot easily be considered by the tracker, and some possible relevant hypotheses will be culled. Such a hypothesis bloom indicates that

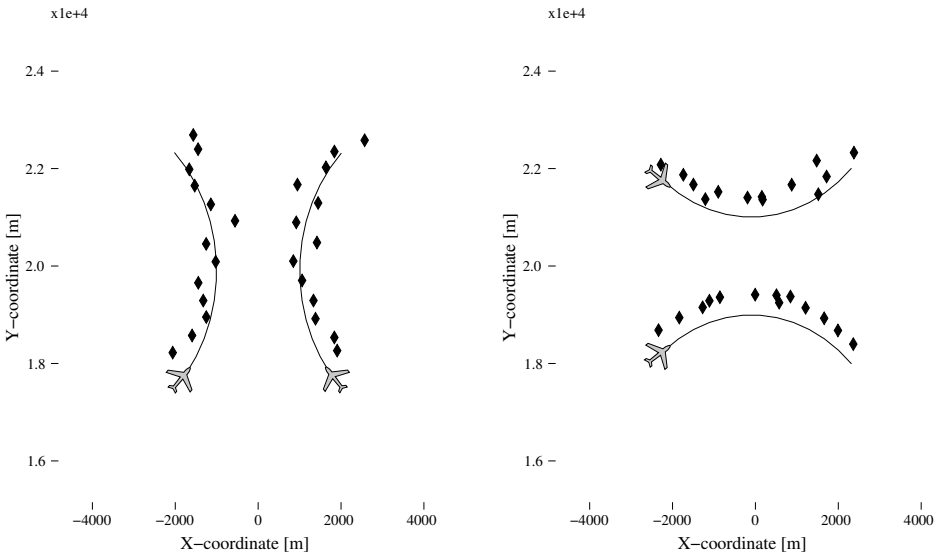

Figure 5.4: Differently oriented manoeuvres.

there is not much to distinguish between the hypotheses anyway, so it will not influence the answer to a great extent.

5.6.2 Manoeuvre orientation

The orientation of manoeuvre with respect to the radar station has an effect on the probabilities obtained. This does follow intuition since the elliptical shape of the measurement noise covariance can make tracks overlap more or less depending on the manoeuvre configuration.

We consider two configurations involving two targets at a similar distance from the radar station, but rotated 90 degrees with respect to the station.

Figure 5.5 expresses the results after 100 runs, and it is apparent that the effect of noise on Figure 5.4*a* causes greater identity uncertainty than in *b*.

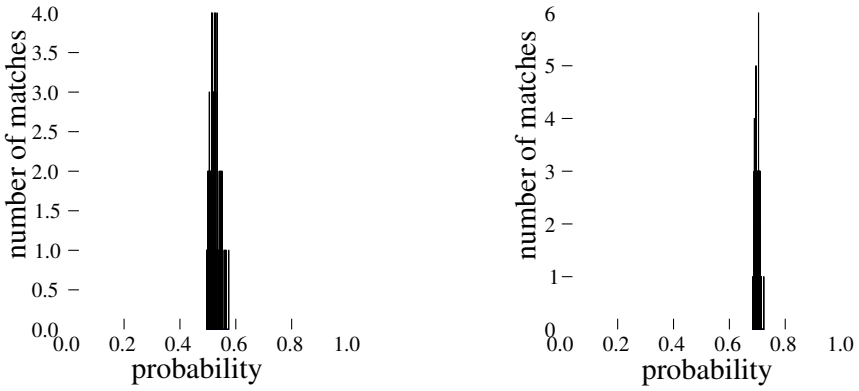

a) b)

Figure 5.5: Oriented manoeuvre results.

5.6.3 Inspection flight pattern

In combat situations a visual inspection is a common manoeuvre. When a aircraft of unknown identity enters the airspace, another aircraft is dispatched to identify the target. This involves close quarters manoeuvring as the inspection aircraft swoops in behind its quarry and there is good chance of target identity confusion during the manoeuvre.

This flight pattern is depicted in Figure 5.6. In this situation we will compare the probabilities obtained of paths bypasses various distances of d.

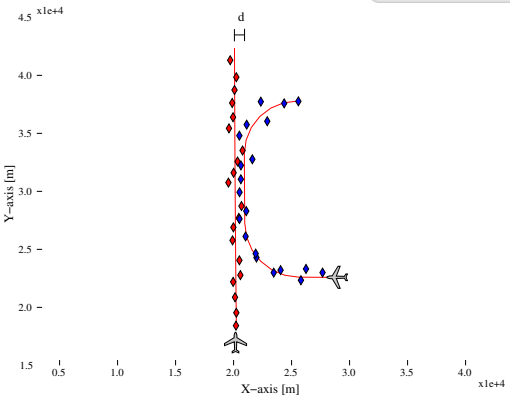

Figure 5.6: Inspection manoeuvre.

Figure 5.7 shows that at $1km$ bypass there is not much certainty to be attached to any identity. For larger values of d the certainty rises until at the farthest bypass of $6km$ the identities most probably remain preserved.

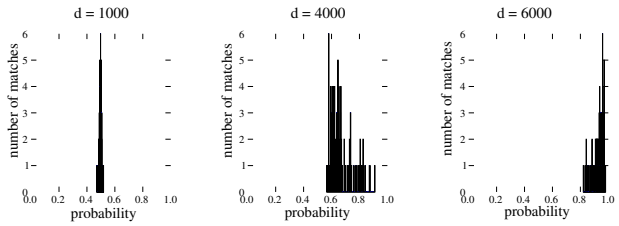

Figure 5.7: Identity confidences of inspection flights for various values of d.

Chapter 6

Conclusion

Radar provides noisy measurements and that can cause uncertainty in the results of a tracker. We were posed with a problem from the industry to determine the identity confidence of a radar track after aircraft interacted closely with each other.

There are various sources of information that should be taken into account: other radar measurements, radar characteristics, aircraft capabilities and track histories. Approaching the problem with radar tracking methodology provides the easiest way for these factors to be integrated easily.

We built a model that represents an aircraft and used it in a Kalman filter to predict aircraft motion. Different kinds of filtering were considered, and the Interacting Multiple Model filter proves to perform the best. This filter mixes a bank of diverse filters and switches between them as the nature of an aircraft's movement changes.

These estimation filters are used in a Multiple Hypothesis Tracker. The tracker considers every possibility of data association and forms a hypothesis for each. MHT is a good way to extract probabilities from a scenario, but it requires careful management of hypotheses to prevent an explosion of possibilities. We have discussed the algorithm in detail, from the theoretical underpinnings to the various implementation details such as culling.

By extending the MHT into an Identity Confidence system and using it ex post facto on tracker output, we have created a robust system that can handle multiple aircraft while incorporating uncertainties of radar environment with ease. Certain issues had to be addressed such as the culling of a large number of hypotheses with equal probabilities. We suggested a method to adjust

the probability of the remaining hypotheses to compensate for the hypotheses deleted.

In order to test the algorithm a simulation system was developed. The results of the Identity Confidence system on a series of benchmarks are encouraging. In the scenario of two crossing aircraft, the confidence probability of a track approaches from unsure to certain as the intersection angle increases. An inspection flight pattern also gives results as expected.

Future work can focus on calibrating the system to match a real world system's operation and on the possiblity of increasing the effectivity of the IMM and Kalman filters. There are many design decisions in a filter that could lead to improved tracking. Improved performance by the use of non-linear filters such as the Particle and Extended Kalman Filters is also something worth exploring further.

Bibliography

[1] The us navy fact file: F-16a/b fighting falcon fighter (date of access 2006-10-01). Technical report. http://www.navy.mil/navydata/fact_display.asp?cid=1100\&tid=1150\&ct=1. 8

[2] Y. Bar-Shalom and X. R. Li. *Multitarget-Multisensor Tracking: Principles and Techniques*. 1995. 3, 12, 16

[3] Y. Bar-Shalom, X. R. Li, and T. Kirubarajan. *Estimation with Applications to Tracking and Navigation*. John Wiley and Sons, Inc, 2001. 21

[4] Y. Bar-Shalom and E. Tse. Tracking in a cluttered environment with probabilistic data association. *Automatica 11*, pages 451–460, 1975. 3, 35

[5] S. Blackman. *Multiple-Target Tracking with Radar Applications*. Artech House. Inc, Dedham, MA, 1986. 3, 12, 14, 16, 37, 39, 44

[6] S. Blackman. Multiple hypothesis tracking for multiple target tracking. *IEEE A+E Systems Magazine: Part 2: Tutorials*, 19(1):5–18, 2003. 3, 45

[7] K. Buckley, A. Vaddiraju, and R. Perry. A new pruning/merging algorithm for mht multitarget tracking. *Proc. Radar-2000*, 2000. 45

[8] I. Cox and S. Hingorani. An efficient implementation of reid's multiple hypothesis tracking algorithm and its evaluation for the purpose of visual tracking. *IEEE Trans. on PAMI*, 18(2):138–150, 1996. 3

[9] M. de Feo, A. Graziano, R. Miglioli, and A. Farina. Immjpda versus mht and kalman filter with nn correlation:performance comparison. *Radar, Sonar and Navigation, IEE Proceedings*, 144(2):49–56, 1997. 36

[10] H. B. de Villiers. Correlation and tracking using multiple radar sensors. Master's thesis, University of Stellenbosch, 2007. 21

[11] F. Gustafsson and A. Isaksson. Best choice of coordinate system for tracking coordinated turns. 1996. 12

[12] S. J. Julier and J. K. Uhlmann. A new extension of the kalman filter to nonlinear systems. *Proceedings- SPIE The International Society for Optical Engineering*, 1997. 16

[13] R. E. Kalman. A new approach to linear filtering and prediction problems. *Transaction of the ASME - Journal of Basic Engineering*, 1960:35–45, 1960. 3, 14

[14] X. R. Li and V. P. Jilkov. volume 4473, pages 423–446, 2001. 12

[15] H. Meikle. *Modern Radar Systems*. Artech House, Inc, Norwood, MA, 2001. 9

[16] D. B. Reid. An algorithm for tracking multiple targets. *IEEE Transactions on Automatic Control*, AC-24(6):843–854, 1979. 3, 39, 44, 45

[17] R. W. Sittler. An optimal data association problem in surveillance theory. *IEEE Transactions on Military Electronics*, volume MIL-8 (Apr):125–139, 1964. 40

Appendix A

Reutech Radar Systems

The following tables tabulate specifications of the radar system used by Reutech Radar Systems.

Kameelperd characteristics	**Value**
Azimuth deviation	0.01222 radians
Range deviation	18 meters
Elevation deviation	n/a
Doppler deviation	n/a
Maximum Range Envelope	65000 meters
Maximum Angle of Sight	0.38921 radians
Maximum Detection Height	8000 meters
Scan Rate / Rotation Rate	4 seconds

Table A.1: Kameelperd sensor parameters

Level	α	β	**Range (m)**	**Azimuth (rad)**
1	1	1	4074	0.4559
2	0.833	0.5	2037	0.2279
3	0.7	0.3	2037	0.2279
4	0.6	0.2	1018.5	0.1140
5	0.524	0.142	679.0	0.0760
6	0.464	0.107	509.2	0.0570
7	0.417	0.083	407.4	0.0456
8	0.378	0.067	339.5	0.0380
9	0.345	0.055	291.0	0.0326
10	0.318	0.055	254.6	0.0285
11	0.295	0.055	254.6	0.0285
12	0.25	0.055	254.6	0.0285
13	0.242	0.055	254.6	0.0285
14	0.228	0.055	254.6	0.0285

Table A.2: Transition table of $\alpha\beta$ parameters used by Reutech Radar Systems.

Appendix B

Software Architecture

The following is a selection and description of the main files in the simulation software developed for this project. Only relevant methods are listed and initializer methods are only mentioned when parameters may need explanation.

B.1 tracegenerator.py

The module generates realistic aircraft traces and converts it to measurements made by a radar site. Currently only supporting 2d movements as required by this project.

B.1.1 class Aircraft:

def __init__(self, start = (0, 0), heading = 0, velocity = 100)

Creates a new aircraft object at specified coordinates heading in a direction at a constant velocity.

def move_straight(self, duration = 40, step = 1)

Moves the aircraft for a duration with measurements made every *step* seconds.

def turn(self, final_heading = pi, turning_g = 1, step = 1):

Turns the aircraft with specified turning g to a final heading, measurements made every *step* seconds.

def hits(self, site = None, height = 4000):

Converts the aircraft trace into measurements made by specified radar site at a specific height.

B.2 radarsite.py

This module describes the radar site and its location.

B.2.1 class RadarSite:

def __init__(self, position = (0, 0, 0), type = 'kameelperd'):

Creates a radar station of specified type at position.

def observation_covariance(self, hit):

Calculates the observation covariance of this radar station for a hit. Used in Kalman filter implementation.

def xyz_to_rangebearing(self, hit):

Converts an xyz measurement into a range bearing tuple.

B.3 kalmanfilter.py, immfilter.py

The Kalman and IMM estimation filters. The Kalman and IMM filter share the same structure, and the IMM filter uses the Kalman filter module extensively internally.

B.3.1 class KalmanFilter and IMMFilter:

def __init__(self, initial_hit = None, mode = 6, processmod = 1.0):

Initializes the filter estimates. *Mode* gives a way to specify whether a filter with 4 states or 6 states are used, and *processmod* is a process noise scaling factor.

def set_noise(self, r):

Updates the observation covariance of the filter or filters in the case of the IMM.

def predict(self, timedelta, processnoise = None):

Predicts the filter estimate a delta *timedelta* into the future. The processnoise parameter is used for prediction using a custom process noise covariance.

def update(self, hit, timedelta = 1.0):

Updates the filter estimates according to a measurement and the delta *timedelta* since last measurement.

B.4 hypothesis.py

This module handles the Hypothesis class and a logical container the HypothesisList class. The HypothesisList contains methods that operates on the collection of hypotheses such as analyses and visualisations.

B.4.1 class Hypothesis:

def __init__(self, container = None):

Initializes the hypothesis as child of the *container* HypothesisList.

def add_track(self, track):

Adds a track to the hypothesis.

def composition(self, hits1, hits2):

Returns a string representation of how the two hit sets are represented in the hypothesis.

def branch(self):

Returns a copy of the hypothesis suitable for hypothesis branching.

B.4.2 class HypothesisList:

def hypo_filter(self, num_missed = 0, num_tracks = 2):

Selects hypotheses with specified number of tracks or number of missed detections.

def find_hypothesis(self, id):

Finds hypothesis with specified *id*.

def find_alternative(self, hits1, hits2):

Finds hypotheses containing a track with the same start and ending in common as the supplied measurement sets *hits1* and *hits2*.

def find_offspring(self, parent):

Finds hypotheses that originally descend from the parent hypothesis.

def new_hypothesis(self):

Creates, registers and returns a new hypothesis.

def equivalent_hypos(self, target):

Find all other hypotheses where the resulting track movements are equivalent to the *target* hypothesis.

def display_hypos(self, hypos, hits1, hits2):

Displays the hypothesis list.

def display_results(self, hits1, hits2, summary = 1, list_relevant = 1, relevant_filter = -1, plot_results = 1, plot_hypo_id = 0, plot_alternative = 0):

Displays the hypothesis list with greater detail.

def trackset_probability(self, *required_tracks):

Accumulate the probability of all hypotheses where the track movements in the required tracks occur.

B.5 mht.py

B.5.1 class MHT:

def __init__(self, hypolist, kalman_mode = 6, filter_type = KalmanFilter, record = False):

Create a Multiple Hypothesis Tracker with specified filter and mode.

def associate(self, scanlist):

Receives a *scanlist* of all measurements received during scan, and then update and create new hypotheses.

def predict(self):

Do filter prediction of all hypotheses.

def manage(self, max_hypos = 20):

Manages hypotheses by culling and redistributing probabilities.

B.6 examplemht.py

Implementation of the MHT identity confidence algorithm using the above modules. As general rule implementation files are prefixed with **example**, while theoretic analyses files are prefixed with **theory**.